Annual Reviews in Control 50 (2020) 345–360

Contents lists available at ScienceDirect

Annual Reviews in Control

journal homepage: www.elsevier.com/locate/arcontrol

Review

Modeling, estimation, and analysis of epidemics over networks: An overview☆

Philip E. Paré [a,*], Carolyn L. Beck [b], Tamer Başar [b]

[a] School of Electrical and Computer Engineering, Purdue University, West Lafayette, IN, United States of America
[b] Coordinated Science Laboratory, University of Illinois at Urbana-Champaign, IL, United States of America

ARTICLE INFO

Keywords:
Epidemic processes
Network-dependent spread
COVID-19
Parameter estimation
Stability analysis
Networked control systems
Nonlinear systems

ABSTRACT

We present and discuss a variety of mathematical models that have been proposed to capture the dynamic behavior of epidemic processes. We first present traditional group models for which no underlying graph structures are assumed, thus implying that instantaneous mixing between all members of a population occurs. Then we consider models driven by similar principles, but involving non-trivial networks where spreading occurs between connected nodes. We present stability analysis results for selected models from both classes, as well as simple least squares approaches for estimating the spreading parameters of the virus from data for each basic networked model structure. We also provide some simulation models. The paper should serve as a succinct, accessible guide for systems and control research efforts toward understanding and combating COVID-19 and future pandemics.

1. Introduction

Numerous examples of natural and engineered systems can be cited that consist of underlying networked components over which dynamical processes evolve or spread. Such examples include the diffusion of infectious disease processes over human contact networks and animal populations, the propagation of peak traffic phenomenon over the transportation infrastructures, the spread of viruses or worms over communication and computer networks, and sharing and re-sharing of posted articles or rumors over social media platforms. Engineered systems are increasingly designed to be smart devices, interconnected over various levels of both local and large-scale networks. Understanding at a fundamental and analytical level how these viral processes evolve across different network structures, the rates at which they may spread, how the occurrence of multiple viral types and multiple network layers affect the spread process dynamics, and how these processes can be suppressed and/or mitigated by employing deliberate control strategies will greatly impact the health, safety and security of a vast variety of interconnected systems around the globe.

We recognize that there is a large and growing body of work on epidemic process dynamics over networks in various disciplines, including but not limited to epidemiology, computer science, complex networks, physics, mathematical biology, applied mathematics, and sociology (Anderson & May, 1992; Boccaletti et al., 2006; Chatterjee & Durrett, 2009; Cherif, 2015; Draief & Massoulie', 2010; Hota & Sundaram, 2019; Kephart & White, 1991; Pires et al., 2018; Rogers, 2003; Rohloff & Başar, 2008; Wan et al., 2007, 2008). However under the current unprecedented situation – a global pandemic resulting from an essentially unknown virus that is threatening the physical and economic well-being of people in every nation, and from which vast amounts of data are being collected – there is an urgent need to develop models, algorithms and analytical tools providing a deeper, data-informed understanding of how epidemic processes spread over networks which may be time-varying and/or consist of multiple layers, and which allow us to design and inform effective control policies to contain and suppress this spread as quickly as possible, and accounting for a variety of trade-offs.

1.1. Historical development

Mathematical models of epidemics and related spread processes have been analyzed and studied for over 200 years, with one of the earliest treatises presented by Bernoulli (1760). The base models

☆ Research supported in part by the C3.ai Digital Transformation Institute sponsored by C3.ai Inc. and the Microsoft Corporation, United States of America, in part by the Jump ARCHES endowment through the Health Care Engineering Systems Center of the University of Illinois at Urbana-Champaign, United States of America, and in part by the National Science Foundation, United States of America, grants NSF-CNS #2028738, NSF-ECCS #2032258, and NSF-ECCS #2032321.

* Corresponding author.
E-mail addresses: philpare@purdue.edu (P.E. Paré), beck3@illinois.edu (C.L. Beck), basar1@illinois.edu (T. Başar).

https://doi.org/10.1016/j.arcontrol.2020.09.003
Received 8 July 2020; Received in revised form 17 September 2020; Accepted 19 September 2020
Available online 25 November 2020
1367-5788/© 2020 Elsevier Ltd. All rights reserved.

for most studies today derive from the so-called *compartment models* proposed by Kermack and McKendrick (1932). These models assume that every subject lies in some segment or compartment of the population at any given time, with these compartments possibly including *susceptible*, *asymptomatic*, *exposed*, *infected* and/or *recovered* population groups. These models further assume that the subjects in the population are well mixed, meaning that the underlying contact network between the subjects is a complete graph. The classic epidemic models are the SIS (susceptible–infected–susceptible) and SIR (susceptible–infected–recovered) models, with increasing interest in SEIRS (susceptible–exposed–infected–recovered–susceptible) models due to COVID-19, which may be more precisely modeled by an SAIRS (susceptible–asymptomatic–infected–recovered–susceptible) model (see (Rothe et al., 2020) and recent articles (Mallapaty, 2020; Yoon & Martin, 2020)). We note that more detailed compartment models may more accurately capture COVID-19, see for example (Giordano et al., 2020); however, such models place requirements on data available to obtain accurate parameter estimation, which may not be generally attainable in the early stages of an outbreak of a previously unknown pathogen, such as with COVID-19 (Silver, 2020; Vrabac, Paré et al., 2020).

Over the past two decades, there has been an intensive and extensive study of epidemic processes over more complex and more realistic network structures than complete graph structures. An early study can be found in (Lajmanovich & Yorke, 1976); recent surveys of the literature on epidemic processes over networks are provided in (Draief & Massoulie', 2010; Pastor-Satorras et al., 2015), and from a controls perspective in (Nowzari et al., 2016).[1] To account for network structure among individuals or subgroups of a population, an agent-based perspective of spread processes is taken, where each agent is represented by a node in the network, and the edges between the nodes represent the strength of the interaction between agents. Agents, or nodes, may represent individuals or subgroups in the population.

Given a total of N agents in a population model, spread processes can be described in a somewhat precise probabilistic framework by large Markov process models (e.g., of dimension 2^N for SIS models and dimension 3^N for SIRS models), which capture the probability of each agent transitioning from susceptible to infected, and/or to recovered states, and back. These probabilities are determined by the infection, healing and/or recovery rates, in addition to the network interconnection structure, and capture the stochastic evolution of such processes. As these models are difficult, if not intractable, to analyze due to their size, it is often assumed that the number of agents is large enough that *mean-field approximations* (MFAs) are valid. For example for SIS models, MFA models are derived by taking expectations over the infection transition rates of the agents and then considering the limiting behavior of the expectation dynamics as the time interval of interest decreases to zero (Mieghem et al., 2009). The details of this process are supplied in Section 3.1.

For agents interconnected via a graph with a weighted adjacency matrix, use of the aforementioned MFA models describing the evolution of an epidemic process over such a graph or network is now largely accepted under the assumption of large and constant agent population size along with additional independence assumptions. Many of these models have been analyzed in some detail and are more accurately viewed as providing upper bounds on the probability of infection of a given agent at any given time (e.g., see (Chatterjee & Durrett, 2009; Mieghem et al., 2009) for discussions and perspectives). A network-dependent ODE SIS model has been studied extensively; the derivation (the details of the subpopulation derivation process are also supplied in Section 3.1) and use of this model can be found in (Fall et al., 2007; Mieghem et al., 2009; Nowzari et al., 2016; Paré et al., 2018), where Paré et al. (2018) also consider time-varying networks. Additionally we note that discrete time versions of these MFA models have also been proposed and studied (Ahn & Hassibi, 2013; Paré et al., 2019; Wang et al., 2003).

The primary goals in most studies of spread process dynamics have been to analyze the system equilibria and determine the convergence behavior of these processes near isolated equilibria. Specifically, conditions for the existence of and convergence to "disease free" (healthy state) or "non-disease free" (endemic state) equilibria have been sought. For the differential equation-based SIS network model, for example, when the condition for "disease free" equilibrium (which depends on the parameters of the model) does not hold, then there exists another equilibrium, i.e., an endemic equilibrium, that is (almost) globally asymptotically stable (Ahn & Hassibi, 2013; Khanafer et al., 2014a, 2014b; Liu et al., 2019; Nowzari et al., 2014). Similar differential equation-based models for SIR processes have also been studied; an analysis of equilibria and convergence properties for static-network SIR models is given in (Mei et al., 2017). Further, exact Markovian process dynamics for SIR epidemics are discussed in (Van Mieghem, 2014).

In the context of the COVID-19 pandemic, there has been an outburst of recent results studying disease spread. Given the magnitude of the results, we briefly mention here some of the preliminary work that employs networked epidemic models. Hota et al. (2020) use a networked SIR model to capture the spread of COVID-19 in southern Europe. The networked SEIR model (Li & Muldowney, 1995) has also been extended to account for transportation (Vrabac, Shang et al., 2020), quarantine (Groendyke & Combs, 2020), and asymptomatic transmission (Arcede et al., 2020).

1.2. Preliminaries

We provide in this sub-section some mathematical preliminaries on matrices and graphs, and also introduce notation commonly used throughout the paper.

Given a vector function of time $x(t)$, we use $\dot{x}(t)$ to indicate its time-derivative. Given two vectors $x_1, x_2 \in \mathbb{R}^n$, $x_1 \geq x_2$ indicates each element of x_1 is greater than or equal to the corresponding element of x_2, $x_1 > x_2$ indicates each element of x_1 is greater than or equal to the corresponding element of x_2 and $x_1 \neq x_2$, and $x_1 \gg x_2$ indicates that each element of x_1 is strictly greater than the corresponding element of x_2. Given a matrix $M \in \mathbb{R}^{n\times n}$, the largest real-valued part of the eigenvalues, or spectral abscissa, of M is denoted $s(M)$ (if the spectrum is possibly complex) and the spectral radius of M is $\rho(M)$. Also, m_{ij} indicates the i,j^{th} entry of M. The notation $\mathrm{diag}(\cdot)$ refers to a diagonal matrix with the argument on the diagonal. The notation $[n]$ refers to the set $\{1,\dots,n\}$. The identity matrix is denoted by I, the all-ones vector is denoted by $\mathbf{1}$, and the all-zeros vector is denoted by $\mathbf{0}$. We assume I, $\mathbf{1}$, and $\mathbf{0}$ have the appropriate dimensions whenever used. We use $E[\cdot]$ to denote the expected value of the argument and $Pr[\cdot]$ to denote the probability of the argument.

Some of the results in the paper rely on properties of Metzler and irreducible matrices. A real square matrix X is called *Metzler* if its off-diagonal entries are nonnegative. We say that a matrix $X \in \mathbb{R}^{n\times n}$ is *reducible* if there exists a permutation matrix T such that $T^{-1}XT = \begin{pmatrix} Y & Z \\ 0 & W \end{pmatrix}$, where Y and W are square matrices, or if $n = 1$ and $X = 0$. A real square matrix is called irreducible if it is not reducible.

Graph theory

A *directed graph*, or *digraph*, is a pair $\mathcal{G} = (\mathcal{V}, \mathcal{E})$, where $\mathcal{V}$ is the set of nodes and $\mathcal{E} \subseteq \mathcal{V} \times \mathcal{V}$ is the set of edges. Given $\mathcal{G}$, we denote an edge from node $i \in \mathcal{V}$ to node $j \in \mathcal{V}$ by (i,j). We say node $i \in \mathcal{V}$ is a neighbor of node $j \in \mathcal{V}$ if and only if $(i,j) \in \mathcal{E}$. When $(i,j) \in \mathcal{E}$ if and only if $(j,i) \in \mathcal{E}$, we call the graph *undirected*. The in-neighbor set of

[1] As the literature in this area is exceedingly large, we cannot provide an overview of all prior research efforts due to space constraints but note that the cited surveys do provide fairly complete coverage of existing results at the time of their publication.

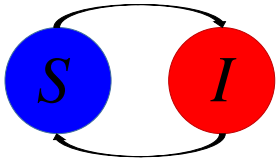

Fig. 1. SIS Model.

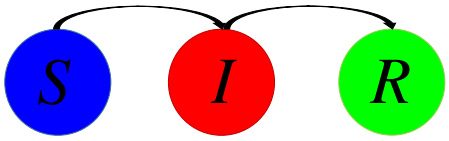

Fig. 2. SIR Model.

node j is defined as $\mathcal{N}_j = \{\, i \mid (i,j) \in \mathcal{E}\}$. For a graph with n nodes, we associate an adjacency matrix $W \in \mathbb{R}^{n\times n}$ with entries $w_{ij} \in \mathbb{R}_{\geq 0}$, where $w_{ij} = 0$ if and only if $(i,j) \notin \mathcal{E}$. For undirected graphs, the adjacency matrix is symmetric.

In a digraph, a directed path is a collection of nodes $\{i_1, \ldots, i_\ell\} \subseteq \mathcal{V}$ such that $(i_k, i_{k+1}) \in \mathcal{E}$ for all $k \in [\ell - 1]$. A digraph is *strongly connected* if there exists a directed path between any two nodes in $\mathcal{V}$. Note that if the digraph is strongly connected, the adjacency matrix is irreducible. A strongly connected component (SCC) of a graph is a subgraph which itself is strongly connected. A path in an undirected graph is defined in a similar manner. We call an undirected graph *connected* if it contains a path between any two nodes in $\mathcal{V}$. A digraph is called *weakly connected* if when every edge in $\mathcal{E}$ is viewed as an undirected edge, the resulting graph is a connected undirected graph. We call a graph, whether it is directed or undirected, *disconnected* if it contains at least two isolated subgraphs. Throughout, when $\mathcal{G}$ is directed, we assume that it is either strongly or weakly connected. When $\mathcal{G}$ is undirected, we assume that it is connected.

1.3. Organization of the paper

In the remainder of the paper we discuss the modeling, analysis and estimation of epidemic dynamics for single group models as well as over networks. We first provide an overview of classic epidemiological compartment models in Section 2; we also discuss modified versions of these models for capturing particular properties of the dynamics of COVID-19 spread processes, namely the increasingly accepted viewpoint that infection may be widely spread from asymptomatic carriers. In Section 3, we present networked versions of the same compartment models, that is, we consider underlying human contact, transportation, and/or community interaction networks that affect the transmission of epidemic processes. In Section 4, we present discrete time versions of the networked models from Section 3 and provide conditions under which the models are well defined. In Section 5, we then discuss stability and convergence of the group models from Section 2. In Section 6, we overview stability/convergence analysis results for the epidemic process models introduced in Sections 3 and 4. Data-based estimation of the relevant parameters defining epidemic process dynamics is presented in Section 7. In Section 8, we present a set of simulations that illustrate the advantages of using the networked models from Section 3 over the group models from Section 2 and discuss the effectiveness of the parameter estimation techniques. Summary and conclusion statements are then given in Section 9.

2. Single group models

The simplest class of mathematical models that captures the spread of epidemics is that which pertains to a single population. In these models separately identified segments of the population reside in one of a fixed number of disease-states at each point in time. For example we might have susceptible and infected (SIS) segments; susceptible, infected, and recovered (SIR and SIRS) segments; susceptible, exposed, infected, and recovered (SEIR and SEIRS) segments; or of more recent interest, susceptible, asymptomatic, infected, and recovered (SAIR and SAIRS) segments. These models are known as group models in compartment form, the simplest of which is the SIS model introduced by Kermack and McKendrick (1932), and given by (see also Fig. 1)

$$\begin{aligned} \dot{S}(t) &= -\beta S(t) I(t) + \gamma I(t), \\ \dot{I}(t) &= \beta S(t) I(t) - \gamma I(t), \end{aligned} \tag{1}$$

where $S(t)$ is the proportion of the population that is susceptible, $I(t)$ is the proportion that is infected, β represents the rate of infection, or contact between susceptible and infected segments of the population, and γ represents the healing or recovery rate of the population.

Such a model assumes a homogeneous population with no vital dynamics, that is, birth and death processes are not included, meaning infection and healing are assumed to occur at faster rates than vital dynamics, and the population size is assumed to remain constant and mix over a trivial network, that is, over a complete graph structure. These statements imply $S(t) + I(t) = 1$, and the population size, which we will denote by N, is constant. Note that $\dot{S} + \dot{I} = 0$, and a certain percentage of those infected will become susceptible again (following recovery). SIS models capture the disease dynamics of recurrent bacterial and fungal infections, such as from Streptoccocus pyogenes or Neisseria gonorrhoeae bacteria, and Trichophyton rubrum (one cause of athlete's foot) or Microsporum canis (one cause of ringworm) fungi, to cite just a few examples.

We next discuss, in the following three subsections, extensions to this simple compartment model accommodating "recovered", "exposed", and "asymptomatic" segments of the population.

2.1. SIR and SIRS models

A slightly more complex model, in which we allow for a state of complete recovery of some duration prior to returning to the susceptible state, is the SIRS model, given by

$$\begin{aligned} \dot{S}(t) &= -\beta S(t) I(t) + \delta R(t), \\ \dot{I}(t) &= \beta S(t) I(t) - \gamma I(t), \\ \dot{R}(t) &= \gamma I(t) - \delta R(t), \end{aligned} \tag{2}$$

where β is the transmission rate parameter for person-to-person contact, γ is the recovery rate, δ is the rate at which immunity recedes following recovery, and $R(t)$ is the recovered proportion of the population. That is, an SIRS model is used when acquired immunity is only temporary, for example, with noroviruses and rotaviruses (i.e., the stomach flu), and some common cold viruses. Alternatively, setting $\delta = 0$ gives us an SIR model (Fig. 2), which captures the dynamics of diseases from which permanent acquired immunity results, such as in the case of the Rubeola virus (measles), varicella-zoster virus (chickenpox), or mumps virus.

To explicitly capture the incubation period from time of exposure to the virus, to the time of expression of symptoms and viral shedding, an SEIR (or SEIRS) model, introduced next, is used.

2.2. SEIR and SEIRS models

The more general SEIRS model, which also allows for the recovered population to be susceptible again after a period of immunity, is

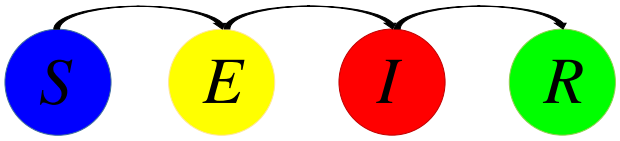

Fig. 3. SEIR Model.

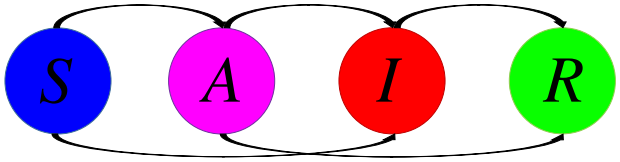

Fig. 4. SAIR Model.

described by the following equations:

$$\begin{aligned}
\dot{S}(t) &= -\beta_E S(t)E(t) - \beta_I S(t)I(t) + \delta R(t),\\
\dot{E}(t) &= \beta_E S(t)E(t) + \beta_I S(t)I(t) - \sigma E(t),\\
\dot{I}(t) &= \sigma E(t) - \gamma I(t),\\
\dot{R}(t) &= \gamma I(t) - \delta R(t),
\end{aligned} \tag{3}$$

where β_E and β_I are the transmission rates from person-to-person contact between susceptible and exposed, and susceptible and infected, respectively. Moreover, σ is the transition rate from exposed to infected, γ is the recovery rate, and δ represents the rate at which immunity recedes. We note that the classic SEIR model (see Fig. 3) has $\beta_E = 0$ (and $\delta = 0$), thus explicitly capturing the delay between time of exposure and when a person becomes simultaneously symptomatic and infectious. For COVID-19, these models have been adapted to capture the state of being both asymptomatic and infectious, leading to SAIR and SAIRS models, described next.

2.3. SAIR and SAIRS models

One SAIRS compartment model, which accommodates asymptomatic states, has the form

$$\begin{aligned}
\dot{S}(t) &= -\beta S(t)(A(t) + I(t)) + \delta R(t),\\
\dot{A}(t) &= \beta q S(t)(A(t) + I(t)) - \sigma A(t) - \kappa A(t),\\
\dot{I}(t) &= \beta(1-q)S(t)(A(t) + I(t)) + \sigma A(t) - \gamma I(t) - \nu I(t),\\
\dot{R}(t) &= \kappa A(t) + \gamma I(t) - \delta R(t),\\
\dot{D}(t) &= \nu I(t),
\end{aligned} \tag{4}$$

where we have further included a compartment capturing death rate due specifically to the disease (D), and again β represents the rate of infection or contact, now amongst susceptible, asymptomatic–infected and infected–symptomatic individuals; σ represents the progression rate from asymptomatic to symptomatic infected; and κ and γ represent the recovery rates for asymptomatic and infected–symptomatic individuals, respectively. That is, this model captures the case of being both asymptomatic and infectious, and recovering without ever exhibiting symptoms. δ represents the rate at which recovered individuals become susceptible again, i.e., lose their immunity to the disease; and ν represents the rate at which infected individuals succumb to the disease. The parameter q, and the $(1-q)$ term, represent the probabilities (or proportions) of susceptible individuals transitioning, respectively, to A and I states from S. If death rate is not included in the model, then we take in (4) $D(0) = 0$ and $\nu = 0$. If further, the acquired immunity is permanent, then we can take $\delta = 0$ in the general SAIRS model (4), leading to a SAIR model (see Fig. 4). The SAIRS (and as a special case SAIR) models may be further generalized by allowing for different β values, or infection rates, between S and A states, and S and I states. Again no general vital dynamics are included in these models. Clearly, to capture an SIRS process from an SAIRS model, we simply set $q = \sigma = \kappa = 0$, with $A(0) = 0$ (Hethcote, 2000; Mena-Lorca & Hethcote, 1992).

SAIR and SAIRS models were first proposed by Grunnill (2018) to capture asymptomatic effects in dengue virus epidemics. With dengue virus strains in humans, being asymptomatic one year may lead to more serious reactions to infections from dengue virus strains in following years. Thus, the SAIR and SAIRS models proposed by Grunnill have different structures than that of (4), which is intended to capture the type of asymptomatic-but-infectious state that may occur with COVID-19.

Remark 1. We note that in all the afore-described compartment models the disease-free state ($I = 0$, $E = I = 0$ in the case of SEIRS, or $A = I = 0$ in the case of SAIRS) is an equilibrium, which is globally asymptotically stable under some conditions on the parameters of the underlying model (for example, for the SIS model, the necessary and sufficient condition is $\beta/\gamma \leq 1$). Since the models represent nonlinear dynamics, there emerges the possibility of additional equilibria; this is indeed the case, with the additional equilibria corresponding to an endemic state, that is $I > 0$ (for example, for the SIS model, the endemic state is $I = 1 - (\gamma/\beta)$, whose positivity and global asymptotic stability is assured when the condition of global asymptotic stability (from any initial condition for I, except $I(0) = 0$) of the disease-free equilibrium does not hold. In Section 5 we provide a more extensive discussion of emerging equilibria for general models and their stability properties. Similarly, in Section 6 we present the analysis for the networked models presented in the next two sections.

3. Networked models—continuous time

As indicated earlier, our main interest is the study of networked models, capturing the scenario where there are numerous groups, or agents, interconnected via a contact graph or more general interconnection network. Such a network is defined by a weighted adjacency matrix, $W = \{w_{ij}\}$, where element w_{ij} quantifies the strength of the connection from agent j to agent i. If we assume as before large and constant agent or group population sizes and specific independence assumptions, then the preceding MFA models describing the evolution of epidemic process dynamics in a single group can be extended to describe the dynamics of epidemic processes evolving over networks of such groups or agents. We refer to these as networked epidemic models.

3.1. SIS model

For an SIS process, denoting the proportion of the subpopulation at node i infected at time t or the probability of node i being infected at any time t by $p_i(t) \in [0,1]$, we have the following differential equation governing the evolution of the p_i's, for $i \in [n]$,

$$\dot{p}_i(t) = (1 - p_i(t))\beta_i \sum_{j=1}^{n} w_{ij} p_j(t) - \gamma_i p_i(t)\,, \tag{5}$$

where $\beta_i > 0$ is the susceptibility rate, w_{ij} are the non-negative, edge weights between the nodes, and $\gamma_i > 0$ is the healing rate, for node i.

For the first interpretation of the state, the model can be derived from a subpopulation perspective as was done by Fall et al. (2007) in the following manner.

With some abuse of notation,[2] let $S_i(t)$ denote the number of susceptible individuals in subpopulation i at time $t \geq 0$, and let $I_i(t)$ denote the number of individuals infected in subpopulation i at time $t \geq 0$. Assume

[2] Note that in the group model for SIS, we used S and I to denote the proportions of the population that are susceptible and infected, whereas in the derivation to follow here we use the i-indexed quantities to denote the number of individuals in each category; since the context is different, this should not cause any confusion.

that the total number of individuals in each subpopulation i, denoted by N_i, is fixed, that is, $S_i(t) + I_i(t) = N_i$, for all $i \in [n]$ and $t \geq 0$. Several parameters are associated with each subpopulation i: curing rate ψ_i, birth rate μ_i, death rate $\bar{\mu}_i$, and infection rates α_{ij} $i, j \in [n]$. Since N_i is constant, $\bar{\mu}_i = \mu_i$. The evolution of the number of infected and susceptible individuals in each subpopulation i is as follows:

$$\begin{aligned}\dot{S}_i(t) &= \mu_i N_i - \bar{\mu}_i S_i(t) + \psi_i I_i(t) - \sum_{j=1}^{n} \alpha_{ij} \frac{S_i(t)}{N_i} I_j(t), \\ &= (\mu_i + \psi_i) I_i(t) - \sum_{j=1}^{n} \alpha_{ij} \frac{S_i(t)}{N_i} I_j(t), \end{aligned} \tag{6}$$

$$\begin{aligned}\dot{I}_i(t) &= -\psi_i I_i(t) - \bar{\mu}_i I_i(t) + \sum_{j=1}^{n} \alpha_{ij} \frac{S_i(t)}{N_i} I_j(t) \\ &= (-\psi_i - \mu_i) I_i(t) + \sum_{j=1}^{n} \alpha_{ij} \frac{S_i(t)}{N_i} I_j(t). \end{aligned} \tag{7}$$

To simplify the model, define the proportion of infected individuals in subpopulation i by

$$p_i(t) = \frac{I_i(t)}{N_i},$$

and let

$$\beta_{ij} = \alpha_{ij} \frac{N_j}{N_i}, \quad \gamma_i = \psi_i + \mu_i,$$

From (7), it follows that

$$\dot{p}_i(t) = -\gamma_i p_i(t) + (1 - p_i(t)) \sum_{j=1}^{n} \beta_{ij} p_j(t), \tag{8}$$

the same as (5) with $\beta_{ij} = \beta_i w_{ij}$. The subpopulation derivation can be used to derive extensions of SIS models for multi-city epidemics (Lewien & Chapman, 2019), competing viruses (Liu et al., 2019), and other compartment models and extensions thereof, as we will see in Section 3.2.

Another way to derive the model in (5) is to use a mean field approximation of a 2^n state Markov chain model that captures the networked SIS dynamics. Van Mieghem et al. (2009) introduce a 2^n-state Markov chain, where each state of the chain, $Y_k(t)$, corresponds to a binary-valued string x of length n, where the ith agent is either infected or susceptible indicated by $x_i = 1$ or $x_i = 0$, respectively, and the state transition matrix, $\bar{Q}$, is defined by

$$\bar{q}_{kl} = \begin{cases} \gamma, & \text{if } x_i = 1, k = l + 2^{i-1} \\ \beta \sum_{j=1}^{n} w_{ij} x_j, & \text{if } x_i = 0, k = l - 2^{i-1} \\ -\sum_{l \neq j} \bar{q}_{jl}, & \text{if } k = l \\ 0, & \text{otherwise,} \end{cases} \tag{9}$$

for $i \in [n]$. Here a virus is propagating over a network structure defined by w_{ij} (non-negative, with $w_{jj} = 0$, for $j \in [n]$), with n agents, β is the homogeneous (same for each node) infection rate, γ is the homogeneous healing rate, and, again, $x_i = 1$ or $x_i = 0$ indicates that the ith agent is either infected or susceptible, respectively. The state vector $y(t)$ is defined by

$$y_k(t) = Pr[Y_k(t) = k], \tag{10}$$

with $\sum_{k=1}^{2^n} y_k(t) = 1$. The Markov chain evolves according to

$$\frac{dy^\top(t)}{dt} = y^\top(t) \bar{Q}. \tag{11}$$

Let $v_i(t) = Pr[X_i(t) = 1]$, where $X_i(t)$ is the random variable representing whether the ith agent is infected (not to be confused with x_i, which is the ith entry of the binary string associated with each state of the 2^n Markov chain). Then

$$v^\top(t) = y^\top(t) M, \tag{12}$$

where $M \in \mathbb{R}^{2^n \times n}$ with the rows being lexicographically-ordered binary numbers, bit reversed.[3] That is, $v_i(t)$ reflects the summation of all probabilities where $x_i = 1$, therefore giving the mean, $E[X_i]$, of the infection, X_i, of agent i. Note that the first chain state of the chain, which corresponds to $x = \mathbf{0}$, the vector of zeros, or the "disease free" equilibrium, for $\gamma > 0$, is the absorbing, or sink, state of the chain. This means that the Markov chain will never escape the state once in it, and further, since it is the only absorbing state the system will converge to the healthy state with probability one (Norris, 1998).

Now consider the probabilities associated with node i being healthy ($X_i = 0$) or infected ($X_i = 1$) at time $t + \Delta t$, for example,

$$\begin{aligned} &Pr(X_i(t + \Delta t) = 0 | X_i(t) = 1, X(t)) = \gamma \Delta t + o(\Delta t), \\ &Pr(X_i(t + \Delta t) = 1 | X_i(t) = 0, X(t)) = \beta \sum_{j=1}^{n} w_{ij} X_j \Delta t + o(\Delta t), \\ &\vdots \end{aligned}$$

Letting Δt go to zero, and taking expectations, lead to

$$\dot{E}(X_i(t)) = E\left((1 - X_i(t)) \beta \sum_{j=1}^{n} w_{ij} X_j(t) \right) - \gamma E(X_i(t)). \tag{13}$$

Using the above equation, the identities $Pr(z) = E(1_z)$, $p_i(t) = Pr(X_i(t) = 1)$, $(1 - p_i(t)) = Pr(X_i(t) = 0)$, and approximating $Pr(X_i(t) = 1, X_j(t) = 1) \approx p_i(t) p_j(t)$ (which again inaccurately assumes independence) gives

$$\dot{p}_i(t) = (1 - p_i(t)) \beta \sum_{j=1}^{n} w_{ij} p_j(t) - \gamma p_i(t),$$

which is the same as (5) for the homogeneous virus case (Pare, 2018).

Note that for both interpretations of the model to be well defined, each state $p_i(t)$ must remain in the domain $[0, 1]$ for all $t \geq 0$. This is indeed the case, as indicated in the following lemma.

Lemma 1. *If $p_i(0) \in [0, 1]$, for all $i \in [n]$, then $p_i(t) \in [0, 1]$, for all $t \geq 0$, $i \in [n]$.*

3.2. SIR model

For an SIR process, denoting the probability of node i being infected and being recovered at any time t by $p_i(t) \in [0, 1]$ and $r_i(t) \in [0, 1]$, respectively, we obtain the following differential equations governing the evolution of the p_i's and r_i's, which is an extension of the networked SIS model (5):

$$\dot{p}_i = (1 - p_i - r_i) \beta_i \sum_{j=1}^{n} w_{ij} p_j - \gamma_i p_i, \tag{14a}$$

$$\dot{r}_i = \gamma_i p_i. \tag{14b}$$

For the networked SIR model to be well defined, the states and their sum must remain in $[0, 1]$. This is indeed the case, as indicated in the following lemma.

Lemma 2. *If $p_i(0)$, $r_i(0)$, $p_i(0)$, $r_i(0) + p_i(0) \in [0, 1]$, for all $i \in [n]$, then $p_i(t), r_i(t), p_i(t) + r_i(t) \in [0, 1]$, for all $t \geq 0$, $i \in [n]$.*

Extensions to the SIR model are possible, some of which will be illustrated later. As one example, Pagliara and Leonard (2020) proposed an SIRI model that allows for partial immunity. Another example, Paré et al. (2019) add a shared resource (water), which can be contaminated, to the SIR model to make a networked SIWR model. We include

[3] Matlab code: $M = fliplr(dec2bin(0 : (2^n) - 1) - '0')$.

below the derivation of this generalized model, paralleling the SIS subpopulation derivation in Section 3.1.

First we consider a network of n nodes that can be interpreted as subpopulations or agents. Specifically, each agent can be infected if one of its neighbors is infected. The neighbor relationships among the n agents are described by an n-vertex directed graph. A directed edge from node j to node i means that agent i can be infected by agent j, i.e., agent j is a neighbor of agent i. Let S_i denote the number of susceptible individuals in subpopulation i, I_i denote the number of infected individuals in subpopulation i, W denote the pathogen concentration in the shared water source, and R_i denote the removed proportion of subpopulation i. We assume a constant subpopulation for each i, that is, $S_i(t) + I_i(t) + R_i(t) = N_i \ \forall i, t \geq 0$. The dynamics proceed similarly to (2):

$$\dot{S}_i(t) = \mu_i N_i - \sum_{j=1}^{n} \alpha_{ij} \frac{S_i(t)}{N_i} I_j(t) - \beta_{w,i} S_i(t) W(t) - \mu_i S_i(t), \tag{15a}$$

$$\dot{I}_i(t) = \sum_{j=1}^{n} \alpha_{ij} \frac{S_i(t)}{N_i} I_j(t) + \beta_{w,i} S_i(t) W(t) - \psi_i I_i(t) - \mu_i I_i(t), \tag{15b}$$

$$\dot{W}(t) = \sum_{j=1}^{n} \alpha_j I_j(t) - \xi W(t), \tag{15c}$$

$$\dot{R}_i(t) = \psi_i I_i(t) - \mu_i R_i(t), \tag{15d}$$

where, for each node i, μ_i is the birth rate and natural death rate, α_{ij} is the node-to-node infection rate (with the understanding that $\alpha_{ij} > 0$ whenever subpopulation j is a neighbor of subpopulation i and $\alpha_{ij} = 0$ otherwise), $\beta_{w,i}$ is the water-to-node infection rate, and ψ_i is the curing or death (from illness, depending on whether the state variable r is interpreted as recovered or removed, i.e., due to death) rate, and α_j is the node-to-water infection rate. Note that in (15) we are considering the rates of change of the numbers of susceptible, infected and recovered/removed, rather than the proportions. For this reason, we require a $\frac{1}{N_i}$ term in the S_i and I_i rate equations. Alternatively, let p_i denote the proportion of the infected subpopulation i (or the probability of infection of agent i), w denote the pathogen concentration in the shared water source (we first assume a single water source), and r_i denote the removed proportion of subpopulation i (or the recovered/removed probability of agent i), that is,

$$p_i = \frac{I_i(t)}{N_i}, \quad r_i = \frac{R_i(t)}{N_i}, \quad w = W.$$

Then the dynamics in (15) can be rewritten as follows:

$$\dot{p}_i = (1 - p_i - r_i)\left(\sum_{j=1}^{n} \beta_{ij} p_j + \beta_{w,i} w\right) - \gamma_i p_i, \tag{16a}$$

$$\dot{r}_i = \psi_i p_i - \mu_i r_i, \tag{16b}$$

$$\dot{w} = \sum_{j=1}^{n} \alpha_j p_j - \xi w, \tag{16c}$$

where

$$\beta_{ij} = \alpha_{ij} \frac{N_j}{N_i}, \quad \alpha_j = \frac{\phi_j}{N_j}, \quad \gamma_i = \psi_i + \mu_i,$$

are the normalized node-to-node infection rates, normalized node-to-water infection rates, and the total decay rates on the normalized infection levels, respectively. Note that the following models can also be derived in a similar manner.

3.3. SEIR model

In a similar fashion to that which was done in Sections 3.1 and 3.2, the group SEIR model can be extended to allow for networked contact structures, as follows:

$$\dot{e}_i = (1 - e_i - p_i - r_i)\left(\sum_{j=1}^{n} \beta_i^E w_{ij} e_j + \sum_{j=1}^{n} \beta_i w_{ij} p_j\right) - \sigma_i e_i, \tag{17a}$$

$$\dot{p}_i = \sigma_i e_i - \gamma_i p_i, \tag{17b}$$

$$\dot{r}_i = \gamma_i p_i, \tag{17c}$$

where e_i is the probability of exposed individuals in subpopulation i; p_i and r_i are as defined in the networked SIR model; σ_i is the rate at which exposed individuals in subpopulation i become infected; β_i^E is the infection rate associated with exposed individuals; and all other parameters are as in the networked SIR model. Here, for simplicity, we ignore the natural death rate. As noted earlier, in classic SEIR models $\beta_i^E = 0$ for all $i \in [n]$, that is, exposed individuals are not contagious.

Lemma 3. *If $e_i(0), p_i(0), r_i(0), p_i(0), e_i(0) + r_i(0) + p_i(0) \in [0, 1]$, for all $i \in [n]$, then $e_i(t), p_i(t), r_i(t), e_i(t) + p_i(t) + r_i(t) \in [0, 1]$, for all $t \geq 0$, $i \in [n]$.*

3.4. SAIR model

The group SAIR model (see (4), with $\delta = 0$) also can be extended to the networked case, to reflect contact network structures:

$$\dot{s}_i(t) = -\beta_i s_i(t)\left(\sum_{j=1}^{n} w_{ij}(a_j(t) + p_j(t))\right), \tag{18a}$$

$$\dot{a}_i(t) = \beta_i q s_i(t)\left(\sum_{j=1}^{n} w_{ij}(a_j(t) + p_j(t))\right) - \sigma_i a_i(t) - \kappa_i a_i(t), \tag{18b}$$

$$\dot{p}_i(t) = \beta_i (1 - q) s_i(t)\left(\sum_{j=1}^{n} w_{ij}(a_j(t) + p_j(t))\right) + \sigma_i a_i(t) - \gamma_i p_i(t), \tag{18c}$$

$$\dot{r}_i(t) = \kappa_i a_i(t) + \gamma_i p(t). \tag{18d}$$

Here, s_i and a_i are the probabilities of an individual in subpopulation i becoming respectively susceptible or asymptomatic, and p_i and r_i admit the same interpretations as in the SIR model. All the parameters are as defined earlier for the group SAIR model. Note that $s_i(t) = 1 - a_i(t) - p_i(t) - r_i(t)$ for all $i \in [n]$.

Lemma 4. *If $a_i(0), p_i(0), r_i(0), p_i(0), a_i(0) + r_i(0) + p_i(0) \in [0, 1]$, for all $i \in [n]$, then $a_i(t), p_i(t), r_i(t), a_i(t) + p_i(t) + r_i(t) \in [0, 1]$, for all $t \geq 0$, $i \in [n]$.*

4. Networked models—discrete time

Disease data is often recorded in epidemiological reports that are compiled at set frequencies, such as weekly (World Health Organization (WHO), b) or daily (Snow, 1855; World Health Organization (WHO), a). The sampling of the epidemics dynamics motivates the use of discrete time models. The following discrete time models are obtained by applying Euler's method (Atkinson, 2008) to the models from Section 3.

4.1. SIS model

Applying Euler's method to (5), we have

$$p_i^{k+1} = p_i^k + h\left((1 - p_i^k)\beta_i \sum_{j=1}^{n} w_{ij} p_j^k - \gamma_i p_i^k\right), \tag{19}$$

where k is the time index and $h > 0$ is the sampling parameter. In matrix form, (19) becomes

$$p^{k+1} = p^k + h((I - P^k)BW - \Gamma)p^k, \tag{20}$$

where $P^k = \text{diag}(p^k)$, $B = \text{diag}(\beta_i)$, W is the matrix of w_{ij}'s, and $\Gamma = \text{diag}(\gamma_i)$. For this model to be well-defined we need the following assumptions.

Assumption 1. For all $i \in [n]$, we have $h\gamma_i < 1$ and $h \sum_{j=1}^{n} \beta_i w_{ij} < 1$.

Lemma 5 (*Paré et al., 2019*). *Consider the model in (19) under Assumption 1. Suppose $p_i^0 \in [0, 1]$ for all $i \in [n]$. Then, for all $k \geq 0$ and $i \in [n]$, $p_i^k \in [0, 1]$.*

Note that if $h = 1$, the model becomes

$$p_i^{k+1} = p_i^k + (1 - p_i^k)\beta_i \sum_{j=1}^{n} w_{ij} p_j^k - \gamma_i p_i^k. \tag{21}$$

The model in (21) was derived by Ahn and Hassibi (2013) via truncation of the higher order terms of a probabilistic discrete-time model. Therefore, there are three different ways to derive the model in (21) as an approximation of the real SIS spread system: (1) using a mean field approximation of a 2^n state continuous time Markov chain model (as explained in Section 3.1), applying Euler's method, and setting the sampling parameter to one, (2) deriving (5) from the subpopulation perspective (as explained in Section 3.1), applying Euler's method, and setting the sampling parameter to one, and 3) through the truncation of the higher order terms of a discrete time probabilistic model. See (Paré et al., 2019, Figure 1) for a visualization of the relationship between the two probabilistic approaches, namely (1) and (3).

4.2. SIR model

Applying Euler's method to (14), we have

$$p_i^{k+1} = p_i^k + h\left((1 - p_i^k - r_i^k)\beta_i \sum_{j=1}^{n} w_{ij} p_j^k - \gamma_i p_i^k\right), \tag{22a}$$

$$r_i^{k+1} = r_i^k - h\gamma_i p_i^k, \tag{22b}$$

where k is the time step and h is the sampling parameter. The SIR discrete-time model can also be expressed in matrix form as follows

$$p^{k+1} = p^k + h\left((I - P^k - R^k)B_d W - \Gamma\right)p^k, \tag{23a}$$

$$r^{k+1} = r^k + h\Gamma p^k. \tag{23b}$$

For this model to be well defined, we also need Assumption 1 to hold.

Lemma 6 (*Hota et al., 2020*). *Consider the model in (22) under Assumption 1. Suppose $s_i^0, p_i^0, r_i^0 \in [0,1]$ and $s_i^0 + p_i^0 + r_i^0 = 1$ for all $i \in [n]$. Then, for all $k \geq 0$ and $i \in [n]$, $s_i^k, p_i^k, r_i^k \in [0,1]$ and $s_i^k + p_i^k + r_i^k = 1$.*

4.3. SEIR model

The corresponding SEIR discrete-time model can be written as

$$e_i^{k+1} = e_i^k + h\left((1 - e_i^k - p_i^k - r_i^k)\left(\sum_{j=1}^{n} \beta_i^E w_{ij} e_j^k + \sum_{j=1}^{n} \beta_i w_{ij} p_j^k\right) - \sigma_i e_i^k\right), \tag{24a}$$

$$p_i^{k+1} = p_i^k + h(\sigma_i e_i^k - \gamma_i p_i^k), \tag{24b}$$

$$r_i^{k+1} = r_i^k + h\left(\gamma_i p_i^k\right), \tag{24c}$$

where k is the time step. The SEIR discrete-time model can also be expressed in matrix form as follows

$$e^{k+1} = e^k + h\left((I - E^k - P^k - R^k)(B^E W e^k + BW p^k) - \Sigma e^k\right), \tag{25a}$$

$$p^{k+1} = p^k + h\left(\Sigma e^k - \Gamma p^k\right), \tag{25b}$$

$$r^{k+1} = r^k + h\left(\Gamma p^k\right), \tag{25c}$$

where $B^E = \mathrm{diag}(\beta_i^E)$ and $\Sigma = \mathrm{diag}(\sigma_i)$.

For the discrete-time model to be well-defined we need the following assumptions.

Assumption 2. For all $i \in [n]$, we have $0 < h\gamma_i < 1$, $0 < h\sigma_i \leq 1$, $0 \leq h(\beta_i^E + \beta_i)\sum_{j=1}^{n} w_{ij} \leq 1$, and $\beta_i^E, \beta_i, w_{ij} \geq 0$ for all $i, j \in [n]$.

Lemma 7 (*Vrabac, Shang et al., 2020*). *Consider the model in (24) under Assumption 2. Suppose $s_i^0, e_i^0, p_i^0, r_i^0 \in [0,1]$, $s_i^0 + e_i^0 + p_i^0 + r_i^0 = 1$ for all $i \in [n]$. Then, for all $k \geq 0$ and $i \in [n]$, $s_i^k, e_i^k, p_i^k, r_i^k \in [0,1]$ and $s_i^k + e_i^k + p_i^k + r_i^k = 1$.*

4.4. SAIR model

The corresponding SAIR discrete-time model can be written as

$$a_i^{k+1} = a_i^k + h\left((1 - a_i^k - p_i^k - r_i^k)\beta_i q \sum_{j=1}^{n} w_{ij}(a_j^k + p_j^k) - \sigma_i a_i^k - \kappa_i a_i^k\right), \tag{26a}$$

$$p_i^{k+1} = p_i^k + h\left((1 - a_i^k - p_i^k - r_i^k)\beta_i (1-q) \sum_{j=1}^{n} w_{ij}(a_j^k + p_j^k) + \sigma_i a_i^k - \gamma_i p_i^k\right), \tag{26b}$$

$$r_i^{k+1} = r_i^k + h\left(\gamma_i p_i^k + \kappa_i a_i^k\right), \tag{26c}$$

where k is the time step. For the discrete-time model to be well defined we need the following assumptions.

Assumption 3. For all $i \in [n]$, we have $\beta_i, w_{ij} \geq 0$, $h\gamma_i \leq 1$, $h(\sigma_i + \kappa_i) \leq 1$, $h(\gamma_i + \kappa_i) \leq 1$, $h\beta_i \sum_{j=1}^{n} w_{ij} \leq 1$, and $h\left(\beta_i(1-q)\sum_{j=1}^{n} w_{ij} + \sigma_i\right) \leq 1$.

Lemma 8. *Consider the model in (26) under Assumption 3. Suppose $s_i^0, a_i^0, p_i^0, r_i^0 \in [0,1]$, $s_i^0 + a_i^0 + p_i^0 + r_i^0 = 1$ for all $i \in [n]$. Then, for all $k \geq 0$ and $i \in [n]$, $s_i^k, a_i^k, p_i^k, r_i^k \in [0,1]$ and $s_i^k + a_i^k + p_i^k + r_i^k = 1$.*

Proof. We prove this result by induction. We assume $s_i^k, a_i^k, p_i^k, r_i^k \in [0,1]$ and $s_i^k + a_i^k + p_i^k + r_i^k = 1$, for the base-case $k = 0$. We follow the proof by showing the induction-step, that is, assuming $s_i^k, e_i^k, p_i^k, r_i^k \in [0,1]$ and $s_i^k + e_i^k + p_i^k + r_i^k = 1$ for all $i \in [n]$, we show that this holds also for $k+1$.

By Assumption 3 and (26), we have,

$$s_i^{k+1} = s_i^k - hs_i^k\beta_i\left(\sum_{j=1}^{n} w_{ij}(a_j^k + p_j^k)\right) \geq s_i^k + h\left[-s_i^k\beta_i\sum_{j=1}^{n} w_{ij}\right] \tag{27}$$

$$= s_i^k\left[1 - h\beta_i\sum_{j=1}^{n} w_{ij}\right] \geq 0. \tag{28}$$

Since, $-hs_i^k\beta_i\left(\sum_{j=1}^{n} w_{ij}(a_j^k + p_j^k)\right) \leq 0$, $s^{k+1} \leq s^k \leq 1$. By Assumption 3 and (26a), $a_i^{k+1} \geq (1 - h(\sigma_i + \kappa_i))a_i^k \geq 0$. Moreover, by the assumption $a_j^k, p_j^k \leq 1$ for all $j \in [n]$, $q \in [0,1]$, Assumption 3, and (26a),

$$a_i^{k+1} \leq a_i^k + s_i^k h\beta_i q \sum_{j=1}^{n} w_{ij} \leq a_i^k + s_i^k \leq 1.$$

By Assumption 3 and (26b), $p_i^{k+1} \geq \left(1 - h\gamma_i\right)p_i^k \geq 0$. Further, by the assumption $a_j^k, p_j^k \leq 1$ for all $j \in [n]$, $q \in [0,1]$, Assumption 3, and (22a),

$$p_i^{k+1} \leq p_i^k + s_i^k h\left(\beta_i(1-q)\sum_{j=1}^{n} w_{ij} + \sigma_i\right) \leq p_i^k + s_i^k \leq 1.$$

By Assumption 2 and (26c), $r_i^{k+1} \geq r_i^k \geq 0$, and $r_i^{k+1} \leq r_i^k + p_i^k + a_i^k$.

Thus, by the principle of mathematical induction we have that, if $s_i^0, a_i^0, p_i^0, r_i^0 \in [0,1]$ and $s_i^0 + a_i^0 + p_i^0 + r_i^0 = 1$ for all $i \in [n]$ then $s_i^k, a_i^k, p_i^k, r_i^k \in [0,1]$ and $s_i^k + a_i^k + p_i^k + r_i^k = 1$ for all $k \in \mathbb{N}$. □

5. Stability analysis—group models

For the single group models of Section 2, or epidemic models that do not entail a network structure, the *basic reproduction number* (or equivalently *basic reproductive number*) (BRN), $\mathcal{R}_0$, serves as a metric that captures the "seriousness" of viral spread; this is considered a fundamental threshold value in epidemiology. The BRN is the expected number of secondary infections arising from one individual throughout their entire infectious period. Thus, for models without network structure, $\mathcal{R}_0$ can be used to evaluate the effectiveness of an action aimed at mitigating the disease spread. To stop the spreading, intuitively one should hold $\mathcal{R}_0 < 1$. As we will see below, because of the nonlinear

nature of spread dynamics we can also allow $\mathcal{R}_0 = 1$. In the sequel we evaluate BRNs and the related property of dynamic stability for the SIS, SIRS, SEIRS and SAIRS group model structures.

5.1. SIS model

For the SIS model of Section 2 it is straightforward to show that the BRN is given by

$$\mathcal{R}_0 = \beta \times 1/\gamma,$$

which is the ratio of the infection to healing rates. The fact that the healthy state (that is, $I = 0$) is globally asymptotically stable if, and only if, $\mathcal{R}_0 \leq 1$ (as also stated in Remark 1) readily follows from rewriting the second equation of (1), under the assumption $S(t) = 1 - I(t)$, as

$$\dot{I}(t) = \beta(1 - I(t))I(t) - \gamma I(t) = \gamma\left(\frac{\beta}{\gamma} - 1\right) I(t) - \beta I^2(t). \tag{29}$$

Note that the right-hand side of this differential equation is bounded above by the linear part; further with the linear part zero (that is, when $\mathcal{R}_0 = 1$) the nonlinear part alone leads to global asymptotic stability, and thus we have that $\mathcal{R}_0 \leq 1$ provides a sufficient condition for global asymptotic stability.[4] Necessity of this condition follows from the fact that when $\mathcal{R}_0 > 1$ the linear part is unstable.

Specifically, what happens if $\mathcal{R}_0 > 1$? In this case, the SIS model has a second equilibrium, the endemic state,

$$I^e = 1 - \frac{\gamma}{\beta},$$

which is clearly positive when $\mathcal{R}_0 > 1$. Defining the equilibrium shifted variable $\tilde{I} := I - I^e$, we arrive at the differential equation (for $\tilde{I}$):

$$\dot{\tilde{I}} = -\beta I^e \tilde{I} - \beta \tilde{I}^2,$$

and from a similar argument as above, it follows that $\tilde{I} = 0$ is globally asymptotically stable, which when translated to the original variable I says that I^e is the globally asymptotically stable endemic equilibrium of the dynamics of the SIS model whenever $\mathcal{R}_0 > 1$ and $I(0) > 0$.

5.2. SIR model

For the SIRS model (2) we continue as in (29) for the SIS model, and set $S(t) = 1 - I(t) - R(t)$, leading to two coupled differential equations:

$$\begin{aligned} \dot{I} &= -(\gamma - \beta)I - \beta RI - \beta I^2, \\ \dot{R} &= \gamma I - \delta R. \end{aligned} \tag{30}$$

When $\delta > 0$, the disease-free equilibrium state can be characterized by $I^e = R^e = 0$, $S^e = 1$ (that is, eventually all recovered become susceptible again, and now remain susceptible since $I^e = 0$). This DFE justifies evaluating stability by linearizing around $I^e = R^e = 0$.

Linearization leads to the 2×2 matrix

$$\begin{bmatrix} \beta - \gamma & 0 \\ \gamma & -\delta \end{bmatrix}.$$

This matrix is Hurwitz if and only if $\beta - \gamma < 0$ and $\delta > 0$. This condition also leads to GAS of the DFE since the two nonlinear terms in the differential equation for I are negative, driving I to zero globally, which also drives R to zero because of the $-\delta R$ term.

If $\delta = 0$ (which gives us the SIR model), note that we cannot make the same argument as above for linearization around $I = R = 0$, since there is now no positive feedback term from the R group to S group. However, for comparison, let us assume for the moment that linearization around $I = R = 0$ makes sense; of course when δ is very small and positive it does, and hence one can consider SIR stability as a limiting case of SIRS stability. Then again we satisfy the Hurwitz condition if and only if $\beta - \gamma < 0$, which is equivalent to $\mathcal{R}_0 < 1$, where $\mathcal{R}_0$ is the BRN defined in the SIS case. This condition also leads to GAS by the argument used in the SIRS case. It is not difficult to see that in this case we can let $\mathcal{R}_0 = 1$ and establish GAS of the disease-free state, since in this case

$$\dot{I} = -\beta RI - \beta I^2;$$

with R being nonnegative, we have GAS.

Now note as a further result of linearization, if the preceding conditions do not hold, that is if $\mathcal{R}_0 > 1$, then for each respective model the disease-free equilibrium is unstable.

Returning to the disease-free equilibrium state for the SIR model (that is, with $\delta = 0$ in SIRS), we have the coupled ODEs:

$$\begin{aligned} \dot{I} &= -(\gamma - \beta)I - \beta RI - \beta I^2, \\ \dot{R} &= \gamma I. \end{aligned} \tag{31}$$

The equilibrium state in this case is $I^e = 0$, $R^e = 1$,[5] with R being positive throughout, except at $I(0) = 0$, and the right-hand-side of the ODE for I being negative whenever $I(0) \neq 0$, and $\mathcal{R}_0 \leq 1$; this immediately leads to the conclusion above, that is the DFE is GAS if and only if $\mathcal{R}_0 \leq 1$.

For SIR, what happens when $\mathcal{R}_0 > 1$? There is no endemic equilibrium, because if the right hand side of the (31) for I is set to zero, for $I \neq 0$ it leads to $I = 1 - R - (\gamma/\beta)$, which is positive only if $R + (\gamma/\beta) < 1$, but there is no such limiting R value since R increases with positive I.

For SIRS, a quick calculation shows that with the right-hand-sides of the coupled ODEs in (30) for I and R set equal to zero, we have a unique solution (for $I \neq 0$):

$$\begin{aligned} R^* &= \frac{\gamma(\beta - \gamma)}{\beta(\gamma + \delta)}, \\ I^* &= \frac{\delta(\beta - \gamma)}{\beta(\gamma + \delta)}, \end{aligned}$$

which are both positive whenever the BRN is larger than 1. Note that $I^* + R^* = 1 - (\gamma/\beta)$, and hence this gives an endemic equilibrium state of S independent of δ. See (Hethcote, 2000) and the references therein for further treatment and discussions on stability and endemic equilibria of SIS and SIR group models.

5.3. SEIR model

For the SEIRS model (3) we continue as in the SIS and SIRS models, and set $S(t) = 1 - E(t) - I(t) - R(t)$, leading to three coupled differential equations:

$$\begin{aligned} \dot{E} &= -(\sigma - \beta_E)E + \beta_I I - \beta_I RE - \beta_I RI - (\beta_E + \beta_I)IE - \beta_E E^2 - \beta_I I^2, \\ \dot{I} &= \sigma E - \gamma I, \\ \dot{R} &= \gamma I - \delta R. \end{aligned} \tag{32}$$

When $\gamma, \delta > 0$, the disease-free equilibrium state can be characterized by $E^e = I^e = R^e = 0$, $S^e = 1$ (that is, eventually all recovered become susceptible again, and now remain susceptible since $E^e = I^e = 0$). This DFE justifies evaluating stability by linearizing around $E^e = I^e = R^e = 0$.

Linearization leads to the 3×3 matrix

$$\begin{bmatrix} \beta_E - \sigma & \beta_I & 0 \\ \sigma & -\gamma & 0 \\ 0 & \gamma & -\delta \end{bmatrix}.$$

[4] Even though this sufficiency holds from all initial conditions for I, what is relevant for the SIS model is the behavior of the system for initial conditions $I(0) \in [0, 1]$.

[5] This not an equilibrium state in the true sense of the notion, since once $R = 1$ it stays there, which is not captured by the smooth right-hand-side of the differential equation above.

With $\gamma, \delta > 0$, this matrix is Hurwitz if and only if $\beta_E - \sigma < -\sigma\beta_I/\gamma$. Therefore, for the SEIRS model we have

$$\mathcal{R}_0 := \frac{-\sigma\beta_I}{\gamma(\beta_E - \sigma)} < 1.$$

This condition leads to GAS of the DFE since the five nonlinear terms in the differential equation for E are negative, driving E to zero globally, which also drives I to zero because of the $-\gamma I$ term; this in turn drives R to zero because of the $-\delta R$ term.

If $\delta = 0$ (which gives us the SEIR model), note that we cannot make the same argument as in the SEIRS case for linearization around $E = I = R = 0$, since there is now no positive feedback term from the R group to S group. However, for comparison, let us assume for the moment that linearization around $E = I = R = 0$ makes sense; of course when δ is very small and positive it does, and hence one can consider SEIR stability as a limiting case of SEIRS stability. Then again, with $\gamma > 0$, we satisfy the Hurwitz condition if and only if $\beta_E - \sigma < -\sigma\beta_I/\gamma$. This condition also leads to GAS by the argument used in the SEIRS case.

We note that stability conditions of the endemic equilibrium for the classic SEIR model were established by Li and Muldowney (1995), which also includes an analysis of the DFE for the classic model.

5.4. SAIR model

We now consider stability of the SAIRS model given by (4) with $D(0) = 0$ and $\nu = 0$; that is we essentially ignore the death rate dynamics in this analysis. As this is a newly proposed model,[6] there is not a previously established BRN analysis. Proceeding as in the SIRS and SEIRS cases we set $S(t) = 1 - A(t) - I(t) - R(t)$, leading to three coupled differential equations:

$$\begin{aligned}
\dot{A} &= -(\sigma + \kappa - \beta q)A - \beta q A^2 - 2\beta q AI - \beta q AR + \beta qI - \beta qI^2 - \beta qIR,\\
\dot{I} &= (\sigma + \beta(1-q))A - \beta(1-q)A^2 - 2\beta(1-q)AI - \beta(1-q)AR\\
&\quad -(\gamma - \beta(1-q))I - \beta(1-q)I^2 - \beta(1-q)IR,\\
\dot{R} &= \kappa A + \gamma I - \delta R.
\end{aligned} \tag{33}$$

Assuming $\delta > 0$ we consider linearization about the DFE point at $A^e = I^e = R^e = 0$, $S^e = 1$, which implies that all recovered become susceptible again and remain susceptible since $I^e = 0$; this gives us the 3×3 matrix

$$\begin{bmatrix} \beta q - \sigma - \kappa & \beta q & 0 \\ \beta(1-q) + \sigma & \beta(1-q) - \gamma & 0 \\ \kappa & \gamma & -\delta \end{bmatrix}.$$

Applying Theorem 4.7 from (Khalil, 2002), straightforward eigenvalue analysis and the Routh–Hurwitz criterion, it can then be seen that the SAIRS model is GAS at the DFE when

$$\mathcal{R}_0 := \max\left(\frac{\beta}{\gamma + \sigma + \kappa}, \frac{\beta(q\gamma + (1-q)\kappa + \sigma)}{\gamma(\sigma + \kappa)}\right) < 1.$$

Analysis of endemic equilibria is noticeably more complex for this model, and to the best of the authors' knowledge has not been completed at this time.

[6] This model was first introduced by the C.L. Beck in the NSF-NeTs COVID-19 Call-to-Arms Workshop sponsored by Ohio State University in April, 2020: see https://sites.google.com/tamu.edu/nets-covid/first-call-to-arms-workshop. The authors have since become aware of a similar model recently proposed by Liu, Wu et al. (2020).

6. Stability analysis—networked models

For networked models, as those in Sections 3 and 4, with an underlying graph structure with nodes and edges, BRN also plays an important role in characterization of the behavior (such as asymptotic stability) of the spread dynamics toward an equilibrium. For such networked models, BRN admits the interpretation of being *the expected number of healthy nodes in a susceptible population that become infected due to the state of infection at neighboring nodes.* We now present results on stability, with connection to the corresponding BRN, for the majority of the networked models presented above, for both continuous-time and discrete-time models.

6.1. SIS models

We first recall in the subsection below the general network structure, also known as the intertwined Markov model.

6.1.1. The n-intertwined Markov model

Following (Khanafer et al., 2016), we describe the networked SIS infection model over a directed graph (digraph) $\mathcal{G} = (\mathcal{V}, \mathcal{E})$ with n nodes, where $\mathcal{V}$ is the set of nodes, and $\mathcal{E}$ is the set of edges. Each node in the network has two states: infected or cured. The curing and infection of a given node $i \in \mathcal{V}$ are described by two independent Poisson processes with rates γ_i and β_i, respectively. Throughout, we assume that $\gamma_i > 0$ and $\beta_i > 0$. The transition rates between the healthy and infected states of a given node's Markov chain depend on its curing rate as well as the infection probabilities among its neighbors. A mean-field approximation is introduced to "average" the effect of infection probabilities of the neighbors on the infection probability of a given node. This approximation yields a dynamical system that describes the evolution of the probability of infection of node $i \in \mathcal{V}$, as described next.

Let $p_i(t) \in [0, 1]$ be the infection probability of node $i \in \mathcal{V}$ at time $t \geq 0$, and let $p(t) = [p_1(t), \ldots, p_n(t)]^T$. Also, let $\Gamma = \text{diag}(\gamma_1, \ldots, \gamma_n)$, $P(t) = \text{diag}(p(t))$, and $B = \text{diag}(\beta_1, \ldots, \beta_n)$. The n-intertwined Markov model is prescribed by the mapping $\Phi : \mathbb{R}^n \to \mathbb{R}^n$, where

$$\dot{p}(t) = \Phi(p(t)) := (W^T B - \Gamma)p(t) - P(t)W^T Bp(t). \tag{34}$$

It is not difficult to see that when $p(0) \in [0, 1]^n$, $p(t) \in [0, 1]^n$, for all $t > 0$.

6.1.2. Equilibrium states of the n-intertwined Markov model

We next focus on characterizing the set of equilibria of the dynamical system (34). The characterization is given in terms of the *basic reproduction number* (BRN), denoted by $\mathcal{R}_0$, introduced earlier in the context of the group SIS model, whose counterpart in the case of networked SIS as above is the expected number of infected nodes produced in a completely susceptible population due to the infection of a neighboring node. For the n-intertwined Markov model, BRN was found in (Mieghem & Omic, 2014) to be equal to $\mathcal{R}_0 = \rho(\Gamma^{-1}W^T B)$. For connected undirected graphs, it is shown in (Van Mieghem et al., 2009) that the disease free equilibrium is the unique equilibrium for the n-intertwined Markov model when $\mathcal{R}_0 \leq 1$. When $\mathcal{R}_0 > 1$, in addition to the disease-free equilibrium, an endemic equilibrium, denoted by $p^\star$, emerges. In fact, it is shown that $p^\star \gg 0$. We call a strictly positive endemic state *strong*. When $p^\star > 0$, we call it a *weak* endemic state. A recursive expression for the endemic state $p^\star$ is provided in (Mieghem & Omic, 2014), which is shown to depend on the problem parameters only: W, γ_i, β_i, $i \in \mathcal{V}$. The steady-state equation evaluated at $p^\star$ will become handy in the derivations to follow and is given by

$$W^T Bp^\star = (I - P^\star)^{-1}\Gamma p^\star, \tag{35}$$

where $P^\star = \text{diag}(p^\star)$. Note that, since we assumed that $\gamma_i > 0$, we have $p_i^\star < 1$, for all $i \in \mathcal{V}$, and $(I - P^\star)^{-1}$ exists.

6.1.3. Stability of the disease free equilibrium

A necessary and sufficient condition for the stability of the disease-free equilibrium is given in the following proposition.

Proposition 1. *(Fall et al., 2007; Lajmanovich & Yorke, 1976) Suppose $\mathcal{G} = (\mathcal{V}, \mathcal{E})$ is a strongly connected digraph. The disease free equilibrium of (5) is asymptotically stable with domain of attraction $[0,1]^n$ if and only if $\mathcal{R}_0 \leq 1$.*

Note that $\mathcal{R}_0$ provides a sharp threshold for the stability of the disease-free equilibrium, as in the group SIS model we discussed earlier.

A similar result holds for the discrete time networked SIS model.

Theorem 1. *(Gracy et al., 2020; Paré et al., 2019) Suppose that Assumption 1 holds and BW is irreducible. The healthy state is the unique equilibrium of (19) if and only if $\rho(I - h\Gamma + hBW) \leq 1$. Further, if $\rho(I - h\Gamma + hBW) \leq 1$ then the healthy state is asymptotically stable with domain of attraction $[0,1]^n$. Finally, if $\rho(I - h\Gamma + hBW) < 1$ then the healthy state is exponentially stable with domain of attraction $[0,1]^n$.*

6.1.4. Existence and stability of an endemic state

In this sub-section, we provide concrete results on local and global asymptotic stability of an endemic state over strongly connected digraphs. We first note, in the proposition below, the existence of a unique endemic state for (34) over strongly connected digraphs.

Proposition 2 (*Fall et al., 2007*)**.** *Let $\mathcal{G} = (\mathcal{V}, \mathcal{E})$ be a strongly connected digraph. Then, a unique strong endemic state $p^\star \gg 0$ exists if and only if $\mathcal{R}_0 > 1$.*

Now the following result on stability of the endemic state is from (Khanafer et al., 2016), which is proven by using positive systems theory and properties of Metzler matrices.

Theorem 2 (*Khanafer et al., 2016*)**.** *Let $\mathcal{G} = (\mathcal{V}, \mathcal{E})$ be a strongly connected digraph, and assume that $p(0) \neq 0$. If $\mathcal{R}_0 > 1$, then the strong endemic state $p^\star$ is globally asymptotically stable, with convergence being exponential locally.*

Existence of an endemic equilibrium has been proven for the discrete time networked SIS model given in (19).

Proposition 3. *(Paré et al., 2019) Suppose that Assumption 1 holds and BW is irreducible. If $\rho(I - h\Gamma + hBW) > 1$ then (19) has two equilibria, $\mathbf{0}$ and p^*, and $p^* \gg \mathbf{0}$.*

Global stability of the endemic equilibrium was recently shown under slightly stronger assumptions by Liu, Cui et al. (2020).

6.1.5. Stability of epidemic dynamics over weakly connected directional graphs

In this section, we discuss results from (Khanafer et al., 2016) on the nature and stability properties of equilibrium states in networked SIS models with a digraph topology. Such a network topology arises in scenarios where there exist connected components that collectively serve as an infection source, but are not affected by the rest of the nodes—scenarios that cannot be captured by strongly connected topologies.

We first introduce some required notation. When the underlying graph $\mathcal{G}$ is weakly connected, its adjacency matrix can be transformed into an upper triangular form using an appropriate re-labeling of the nodes. Assuming that $\mathcal{G} = (\mathcal{V}, \mathcal{E})$ contains N strongly connected components (SCCs), we have

$$W = \begin{bmatrix} W_{11} & W_{12} & \cdots & W_{1N} \\ 0 & W_{22} & W_{23} & \cdots \\ \vdots & \ddots & \ddots & \ddots \\ 0 & \cdots & 0 & W_{NN} \end{bmatrix},$$

where W_{ii} are irreducible for all $i \in [N]$, and, hence, correspond to SCCs in $\mathcal{G}$ in Berman and Plemmons (1994); the matrices W_{ij}, $j \neq i$, however, are not necessarily irreducible. We denote an SCC of $\mathcal{G}$ by $\mathcal{G}_i = (\mathcal{V}_i, \mathcal{E}_i)$, $i \in [N]$, where $\cup_{i=1}^N \mathcal{V}_i = \mathcal{V}$ and $\cup_{i=1}^N \mathcal{E}_i = \mathcal{E}$. For each $i \in [N]$, we introduce the positive diagonal matrices γ_i, B_i which contain, respectively, the curing and infection rates of the nodes in $\mathcal{V}_i$. We introduce the partial order '$\prec$' among SCCs, and write $\mathcal{G}_i \prec \mathcal{G}_j$, for some $i, j \in [N]$, if there is a directed path from $\mathcal{G}_i$ to $\mathcal{G}_j$ but not vice versa.

For a given $i \in [N]$, we denote the state of the nodes in $\mathcal{G}_i$ by $q_i \in \mathbb{R}^{|\mathcal{V}_i|}$ and the state of the kth node in $\mathcal{V}_i$ by $q_{i,k} \in \mathbb{R}$. The state, p, of the entire network is given by $p = [q_1^T, \ldots, q_N^T]$. Let $c_i = \sum_{j \neq i} W_{ji}^T B_j q_j \in \mathbb{R}^{|\mathcal{V}_i|}$, $i \in [N]$, be the input infection from the nodes in $\mathcal{G} \backslash \mathcal{G}_i$. We can now write the dynamics of the nodes in $\mathcal{G}_i$, $i \in [N]$, given by the mapping $\tilde{\Phi}_i : \mathbb{R}^{|\mathcal{V}_i|} \times \mathbb{R}^{|\mathcal{V}_i|} \to \mathbb{R}^{|\mathcal{V}_i|}$, as

$$\dot{q}_i = \tilde{\Phi}_i(q_i, c_i) := (W_i^T B_i - \gamma_i) q_i - Q_i W_i^T B_i q_i + (I - Q_i) c_i, \tag{36}$$

where $Q_i = \mathrm{diag}(q_i)$. When an SCC comprises a single node, $W_i^T B_i - \gamma_i$ is equal to $-\gamma_i$. In what follows, we say $\mathcal{G}_i$ is stable to mean that the dynamics (36) are stable. When an endemic state $p^\star$ emerges over the graph $\mathcal{G}$, we call the steady-state of q_i an endemic state of $\mathcal{G}_i$, and we denote it by $q_i^\star$. Hence, the endemic state emerging over the entire network is given by $p^\star = [q_1^{\star T}, \ldots, q_N^{\star T}]^T$.

The following result from (Khanafer et al., 2016) now provides a complete description of the stability properties of the networked SIS model with weakly connected digraph topology. Here again the BRN, this time defined for each subgraph, plays an important role in global asymptotic stability (GAS) of disease-free and endemic equilibria.

Theorem 3 (*Khanafer et al., 2016*)**.** *Let $\mathcal{G} = (\mathcal{V}, \mathcal{E})$ be a weakly connected digraph consisting of N SCCs ordered as $\mathcal{G}_1 \prec \ldots \prec \mathcal{G}_N$. Let $\mathcal{R}_0^i := \rho(\gamma_i^{-1} W_i^T B_i)$ be the BRN corresponding to $\mathcal{G}_i$. Assume that $q_i(0) \neq 0$ for all $i \in [n]$. :*

1. *If $\mathcal{R}_0^i \leq 1$ for all $i \in [N]$, then the disease-free equilibrium is GAS.*
2. *If $\mathcal{R}_0^k > 1$ for some $k \in [N]$, and $\mathcal{R}_0^i \leq 1$ for $i \in [k-1]$, then the endemic state $p^\star = [0, \ldots, 0, q_k^{\star T}, \ldots, q_N^{\star T}]^T$ is GAS.*

6.2. SIR models

We first consider the continuous time model in (14). We appeal to a result by Mei et al. (2017) which assumes homogeneous virus spread. Recall that $s_i(t) = 1 - p_i(t) - r_i(t)$ for all $i \in [n]$.

Theorem 4 (*Mei et al., 2017*)**.** *Consider the model in (14) with homogeneous spread and $\beta > 0$ and $\gamma > 0$, W irreducible, $p_i(0) > 0$ for some i, and $s_i(0) > 0$ for all $i \in [n]$. For $t \geq 0$, let $\lambda_{\max}(t)$ and $v_{\max}(t)$ be the dominant eigenvalue of the non-negative matrix $\mathrm{diag}(s(t))W$ and the corresponding normalized left eigenvector, respectively. Then, for all $i \in [n]$,*

(1) $t \to s_i(t)$ is monotonically decreasing, for all $t \geq 0$,
(2) the set of equilibrium points is the set of pairs $(s^*, \mathbf{0})$, for any $s^* \in [0,1]^n$,
(3) $\lim_{t \to \infty} p_i(t) = 0$,
(4) there exists $\bar{t}$ such that $\beta \lambda_{\max}(t) < \gamma$ for all $t \geq \bar{t}$, and the weighted average $t \to v_{\max}(\bar{t})^\top x(t)$, for $t \geq \bar{t}$, is monotonically and exponentially decreasing to zero.

To facilitate the discrete time SIR result we write/reiterate the dynamics in (22) as

$$s_i^{k+1} = s_i^k + h\Big[-s_i^k \sum_{j=1}^n \beta_i w_{ij} p_j^k\Big], \tag{37a}$$

$$p_i^{k+1} = p_i^k + h\Big[s_i^k \sum_{j=1}^n \beta_i w_{ij} p_j^k - \gamma_i p_i^k\Big], \tag{37b}$$

$$r_i^{k+1} = r_i^k + h\gamma_i p_i^k. \tag{37c}$$

Theorem 5 (*Hota et al., 2020*). *Consider the model in (22) with Assumption 1, $h\gamma_i > 0$ for all $i \in [n]$, and $p_i^0 > 0$ for some i. Then, for all $i \in [n]$,*

(1) $s_i^{k+1} \leq s_i^k$, for all $k \geq 0$,
(2) $\lim_{k\to\infty} p_i^k = 0$,
(3) $\rho(I + h\text{diag}(s^k)BW - h\Gamma)$ is monotonically decreasing as a function of k, $k \geq 0$,
(4) there exists $\bar{k}$ such that $\rho(I + h\text{diag}(s^k)BW - h\Gamma) < 1$ for all $k \geq \bar{k}$, and
(5) there exists $\bar{k}$, such that p_i^k converges linearly to 0 for all $k \geq \bar{k}$.

6.3. SEIR models

To facilitate the following result we write/reiterate the dynamics in (24a)–(24c) as

$$s_i^{k+1} = s_i^k + h\left[-s_i^k\left(\sum_{j=1}^n \beta_i^E w_{ij} e_j^k + \sum_{j=1}^n \beta_i w_{ij} p_j^k\right)\right], \tag{38a}$$

$$e_i^{k+1} = e_i^k + h\left[s_i^k\left(\sum_{j=1}^n \beta_i^E w_{ij} e_j^k + \sum_{j=1}^n \beta_i w_{ij} p_j^k\right) - \sigma_i e_i^k\right], \tag{38b}$$

$$p_i^{k+1} = p_i^k + h[\sigma_i e_i^k - \gamma_i p_i^k], \tag{38c}$$

$$r_i^{k+1} = r_i^k + h\gamma_i p_i^k, \tag{38d}$$

Let $\lambda_{max}^{M_k}$ be the dominant eigenvalue of M_k, where M_k is defined as

$$M_k = \begin{bmatrix} (I + h\text{diag}(s^k)B^E W - h\Sigma) & h\text{diag}(s^k)BW \\ h\Sigma & (I - h\Gamma) \end{bmatrix},$$

appealing to the notation from (25).

Theorem 6 (*Vrabac, Shang et al., 2020*). *Consider the model in (24) under Assumption 2. Suppose $s_i^0, e_i^0, p_i^0, r_i^0 \in [0,1]$, $s_i^0 + e_i^0 + p_i^0 + r_i^0 = 1$ for all $i \in [n]$ and $p_i^0 > 0$ for some i. Then, for all $k \geq 0$ and $i \in [n]$,*

(1) $s_i^{k+1} \leq s_i^k$,
(2) $\lim_{k\to\infty} e_i^k = 0$ and $\lim_{k\to\infty} p_i^k = 0$,
(3) $\lambda_{\max}^{M_k}$ is monotonically decreasing as a function of k,
(4) there exist a $\bar{k}$ such that $\lambda_{\max}^{M_k} < 1$ for all $k \geq \bar{k}$,
(5) there exists $\bar{k}$, such that p_i^k converges linearly to 0 for all $k \geq \bar{k}$ and $i \in [n]$.

7. Estimation of epidemic parameters

In this section we discuss estimating the parameters of the networked models introduced in Section 4 from data. There have been numerous studies focused on estimating parameters for epidemic process models (see for example (Roosa & Chowell, 2019) and the references therein; note also (Cheynet, 2020)), with recent work focused on constructing COVID-19 models from data (for example, a recent but very short list includes (Anastassopoulou et al., 2020; Bertozzi et al., 2020; Giordano et al., 2020). Much of the prior work provides estimated parameters for group models or considers large probabilistic models, and does not directly address estimation of parameters for epidemic processes over networks. To the best of the authors' knowledge, the first work to consider estimation of networked epidemic models is presented in (Paré et al., 2019).

7.1. SIS model

Following the approach taken by Paré et al. (2019) and Vrabac, Paré et al. (2020), we can rewrite the networked SIS dynamics in (20) as a linear relationship between observed data and unknown parameters β_i, δ_i in the form

$$\begin{bmatrix} p_i^1 - p_i^0 \\ \vdots \\ p_i^T - p_i^{T-1} \end{bmatrix} = \boldsymbol{\Phi}_i \begin{bmatrix} \beta_i \\ \gamma_i \end{bmatrix}, \tag{39}$$

where the matrix $\boldsymbol{\Phi}$ is defined as

$$\boldsymbol{\Phi}_i = \begin{bmatrix} hs_i^0 \sum_{j\in\mathcal{N}_i} w_{ij} p_j^0 & -hp_i^0 \\ \vdots & \vdots \\ hs_i^{T+1} \sum_{j\in\mathcal{N}_i} w_{ij} p_j^{T-1} & -hp_i^{T-1} \end{bmatrix}, \tag{40}$$

and $s_i^k = (1 - p_i^k)$ for the SIS model. The least squares estimates $\hat{\beta}_i$ and $\hat{\gamma}_i$ can be computed directly using the pseudoinverse of $\boldsymbol{\Phi}_i$ for all $i \in [n]$. If $\boldsymbol{\Phi}_i$ is full column rank, $\hat{\beta}_i$ and $\hat{\gamma}_i$ are unique. We state the following result introduced in preliminary form in (Paré et al., 2019); a proof can be found in (Vrabac, Paré et al., 2020).

Theorem 7 (*Vrabac, Paré et al., 2020*). *Consider the model in (19). Assume that p_j^k, for all $j \in \mathcal{N}_i \cup \{i\}$, $k \in [T-1] \cup \{0\}$, p_i^T, W, and h are known. Then, the parameters of the spreading process for node i can be identified uniquely if and only if $T > 1$, and there exist $k_1, k_2 \in [T-1] \cup \{0\}$ such that*

$$p_i^{k_1}(1 - p_i^{k_2}) \sum_{j=1}^n w_{ij} p_j^{k_2} \neq p_i^{k_2}(1 - p_i^{k_1}) \sum_{j=1}^n w_{ij} p_j^{k_1}. \tag{41}$$

Similarly for homogeneous spread parameters, that is, where $\beta_i = \beta$ and $\gamma_i = \gamma$ for all $i \in [n]$, by rewriting the SIS dynamics as

$$\begin{bmatrix} p^1 - p^0 \\ \vdots \\ p^T - p^{T-1} \end{bmatrix} = h\boldsymbol{\Phi} \begin{bmatrix} \beta \\ \gamma \end{bmatrix}, \tag{42}$$

where the matrix $\boldsymbol{\Phi}$ is defined as

$$\boldsymbol{\Phi} := \begin{bmatrix} (I - P^0)W p^0 & -p^0 \\ \vdots & \vdots \\ (I - P^{T-1})W p^{T-1} & -p^{T-1} \end{bmatrix}, \tag{43}$$

if $\boldsymbol{\Phi}$ is full column rank, we can uniquely recover β and γ. This leads us to the following result.

Theorem 8 (*Vrabac, Paré et al., 2020*). *Consider the model in (20) with homogeneous spread, that is, $\beta_i = \beta$ and $\gamma_i = \gamma$ for all $i \in [n]$. Assume that W, p^k, for all $k \in [T] \cup \{0\}$, and h are known. Then, β and γ can be identified uniquely if and only if $T > 0$, and there exist $i, j \in [n]$ and $k_1, k_2 \in [T-1] \cup \{0\}$ such that*

$$p_i^{k_1} g_j(p^{k_2}) \neq p_j^{k_2} g_i(p^{k_1}), \tag{44}$$

where $g(p^k) := (I - P^k)W p^k$.

7.2. SIR model

The straightforward least squares estimation approach described for the networked SIS model in the preceding section can be easily extended to the networked SIR, SEIR and SAIR models. To estimate the spreading parameters for the discrete time, heterogeneous SIR model discussed in Section 4.2 we can rewrite the dynamics given by (22) as

$$\begin{bmatrix} p_i^1 - p_i^0 \\ \vdots \\ p_i^T - p_i^{T-1} \\ r_i^1 - r_i^0 \\ \vdots \\ r_i^T - r_i^{T-1} \end{bmatrix} = P_i \begin{bmatrix} \beta_i \\ \gamma_i \end{bmatrix}, \text{ where } P_i = \begin{bmatrix} \boldsymbol{\Phi}_i \\ \Gamma_i \end{bmatrix}, \tag{45}$$

with $\boldsymbol{\Phi}_i$ defined as in (40), recalling that $s_i^k = 1 - p_i^k - r_i^k$ for the SIR model, and with

$$\Gamma_i = \begin{bmatrix} 0 & hp_i^0 \\ \vdots & \vdots \\ 0 & hp_i^{T-1} \end{bmatrix}. \tag{46}$$

The least squares estimates $\hat{\beta}_i$ and $\hat{\gamma}_i$ can again be computed using the pseudoinverse of P_i for all $i \in [n]$; if P_i is full column rank we have unique solutions.

Theorem 9 (*Vrabac, Shang et al., 2020*). *Consider the model in (22). Assume that s_i^k, p_j^k, r_i^k, for all $j \in \mathcal{N}_i \cup \{i\}, k \in [T-1] \cup \{0\}$, p_i^T, r_i^T, and h are known. Then, the parameters of the spreading process for node i can be identified uniquely if and only if $T > 0$, and there exist $k_1, k_2 \in [T-1] \cup \{0\}$ such that*

$$p_i^{k_1} \neq 0 \text{ and } s_i^{k_2} \sum_{j \in \mathcal{N}_i} a_{ij} p_j^{k_2} \neq 0. \tag{47a}$$

7.3. SEIR model

To estimate the spreading parameters for the discrete time SEIR model from Section 4.3 we continue to extend the least squares approach and rewrite the dynamics in (24) as

$$\begin{bmatrix} e_i^1 - e_i^0 \\ \vdots \\ e_i^T - e_i^{T-1} \\ p_i^1 - p_i^0 \\ \vdots \\ p_i^T - p_i^{T-1} \\ r_i^1 - r_i^0 \\ \vdots \\ r_i^T - r_i^{T-1} \end{bmatrix} = P_i^E \begin{bmatrix} \beta_i^E \\ \beta_i \\ \sigma_i \\ \gamma_i \end{bmatrix}, \text{ where } P_i^E = \begin{bmatrix} \Phi_i^E \\ \Sigma_i^E \\ \Gamma_i^E \end{bmatrix}, \tag{48}$$

with

$$\Phi_i^E = \begin{bmatrix} hs_i^0 \sum_{j \in \mathcal{N}_i} w_{ij} e_j^0 & hs_i^0 \sum_{j \in \mathcal{N}_i} w_{ij} p_j^0 & -he_i^0 & 0 \\ \vdots & \vdots & \vdots & \vdots \\ hs_i^{T-1} \sum_{j \in \mathcal{N}_i} w_{ij} e_j^{T-1} & hs_i^{T-1} \sum_{j \in \mathcal{N}_i} w_{ij} p_j^{T-1} & -he_i^{T-1} & 0 \end{bmatrix}, \tag{49}$$

$$\Sigma_i^E = \begin{bmatrix} 0 & 0 & he_i^0 & -hp_i^0 \\ \vdots & \vdots & \vdots & \vdots \\ 0 & 0 & he_i^{T-1} & -hp_i^{T-1} \end{bmatrix}, \text{ and} \tag{50}$$

$$\Gamma_i^E = \begin{bmatrix} 0 & 0 & 0 & hp_i^0 \\ \vdots & \vdots & \vdots & \vdots \\ 0 & 0 & 0 & hp_i^{T-1} \end{bmatrix}, \tag{51}$$

recalling that $s_i^k = 1 - e_i^k - p_i^k - r_i^k$ for the SEIR model.

The least squares estimates $\hat{\beta}_i^E$, $\hat{\beta}_i$, $\hat{\sigma}_i$, and $\hat{\gamma}_i$ are again computed using the pseudoinverse of P_i^E for all i.

Theorem 10 (*Vrabac, Shang et al., 2020*). *Consider the model in (24). Assume that $s_i^k, e_j^k, p_j^k, r_i^k$, for all $j \in \mathcal{N}_i \cup \{i\}, k \in [T-1] \cup \{0\}$, e_i^T, p_i^T, r_i^T, and h are known. Then, the parameters of the spreading process for node i can be identified uniquely if and only if $T > 1$, and there exist $k_1, k_2, k_3, k_4 \in [T-1] \cup \{0\}$ such that*

$$p_i^{k_1} \neq 0, \; e_i^{k_2} \neq 0, \tag{52a}$$

$$g_i^{k_3}(e^{k_3}) g_i^{k_4}(p^{k_4}) \neq g_i^{k_4}(e^{k_4}) g_i^{k_3}(p^{k_3}), \tag{52b}$$

where $g_i^k(x) = s_i^k \sum_{j \in \mathcal{N}_i} a_{ij} x_j$ which only uses the entries x_j which $j \in \mathcal{N}_i$.

7.4. SAIR model

Finally, to estimate the spreading parameters $(\beta_i, \sigma_i, \gamma_i, \kappa_i)$ for the discrete time SAIR model from Section 4.4 we first assume q is known, and then rewrite (26) as

$$\begin{bmatrix} a_i^1 - a_i^0 \\ \vdots \\ a_i^T - a_i^{T-1} \\ p_i^1 - p_i^0 \\ \vdots \\ p_i^T - p_i^{T-1} \\ r_i^1 - r_i^0 \\ \vdots \\ r_i^T - r_i^{T-1} \end{bmatrix} = P_i^A \begin{bmatrix} \beta_i \\ \sigma_i \\ \gamma_i \\ \kappa_i \end{bmatrix}, \text{ where } P_i^A = \begin{bmatrix} \Phi_i^A \\ \Sigma_i^A \\ \Gamma_i^A \end{bmatrix}, \tag{53}$$

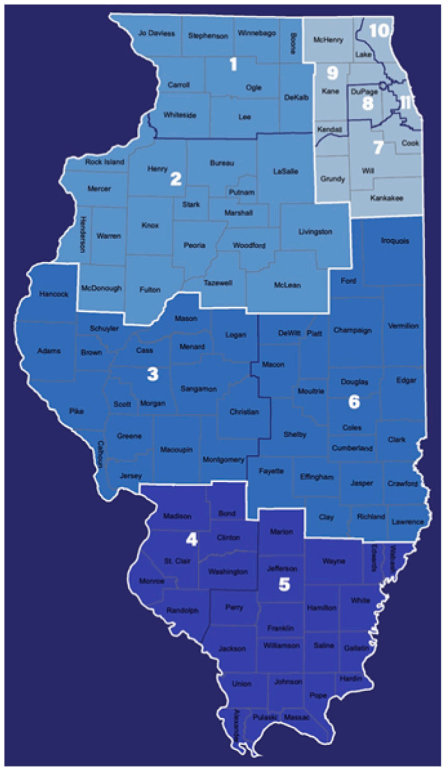

Fig. 5. Health regions from the Restore Illinois Plan (Illinois Department of Public Health, 2020).

with

$$\Phi_i^A = \begin{bmatrix} hq\left(s_i^0 \sum_{j=1}^n w_{ij} a_j^0 + s_i^0 \sum_{j=1}^n w_{ij} p_j^0\right) & -ha_i^0 & 0 & -ha_i^0 \\ \vdots & \vdots & \vdots & \vdots \\ hq\left(s_i^{T-1} \sum_{j=1}^n w_{ij} a_j^{T-1} + s_i^{T-1} \sum_{j=1}^n w_{ij} p_j^{T-1}\right) & -ha_i^{T-1} & 0 & -ha_i^{T-1} \end{bmatrix}, \tag{54}$$

$$\Sigma_i^A = \begin{bmatrix} h(1-q)\left(s_i^0 \sum_{j=1}^n w_{ij} a_j^0 + s_i^0 \sum_{j=1}^n w_{ij} p_j^0\right) & ha_i^0 & -hp_i^0 & 0 \\ \vdots & \vdots & \vdots & \vdots \\ h(1-q)\left(s_i^{T-1} \sum_{j=1}^n w_{ij} a_j^{T-1} + s_i^{T-1} \sum_{j=1}^n w_{ij} p_j^{T-1}\right) & ha_i^{T-1} & -hp_i^{T-1} & 0 \end{bmatrix}, \tag{55}$$

and

$$\Gamma_i^A = \begin{bmatrix} 0 & 0 & hp_i^0 & ha_i^0 \\ \vdots & \vdots & \vdots & \vdots \\ 0 & 0 & hp_i^{T-1} & ha_i^{T-1} \end{bmatrix}, \tag{56}$$

recalling that $s_i^k = 1 - a_i^k - p_i^k - r_i^k$ for the SAIR model.

In this case, we compute the least squares estimates $\hat{\beta}_i$, $\hat{\sigma}_i$, $\hat{\gamma}_i$ and $\hat{\kappa}_i$ using the pseudoinverse of P_i^A for all i. If we do not know q and relax the assumption that this is known, we no longer have a straightforward linear dependency on the unknown parameters (including q). The details of this case are not provided herein.

8. Simulations

For the simulations, we draw from the Restore Illinois Plan (Illinois Department of Public Health, 2020). However, note that we only employ simulated data to illustrate the value of the models. Applying the estimation techniques from Section 7 to real data is ongoing work.

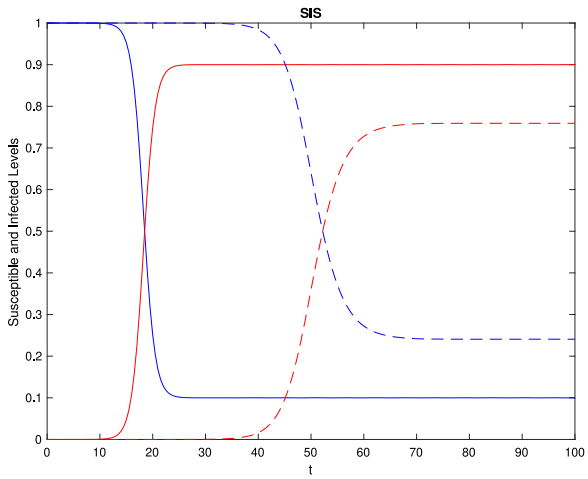

Fig. 6. SIS simulation results. Blue and red represent susceptible and infected, respectively. The solid lines are the states of the group model in (1) and the dashed lines indicate the average states of the networked model in (5). Note that the group model over-predicts the outbreak.

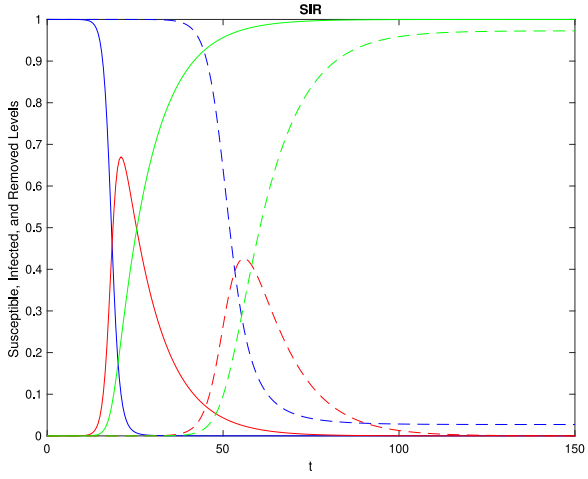

Fig. 7. SIR simulation results. Blue, red, and green represent susceptible, infected, and recovered (or removed), respectively. The solid lines are the states of the group model in (2) and the dashed lines represent the average states of the networked model in (14).

It is easy to aggregate the state of Illinois into one large group, but doing so ignores the nuances of the political and economical structures as well as the non-uniform population distribution across the state. Relying on this setting, we compare the models from Sections 2 and 3, that is, treating the state as one group versus splitting it into different regions. For the more-refined, networked model we use the eleven health regions from the Restore Illinois Plan; see Fig. 5. The adjacency matrix used is a nearest-neighbor relationship between the eleven regions, that is, if two regions share a border, they are connected. Further, we include a connection between regions 3 and 11, given the strong connections between Springfield, which is the capital of the state, and Chicago, the largest city in the state. We also include self loops for each region. Each nonzero entry of the adjacency matrix W is set to $\frac{1}{n}$, where n is the number of regions, taken to be equal to 11.

The group model ignores the network structure and assumes a full connected underlying graph between the nodes. That is, when $W = \frac{1}{n}\mathbf{1}\mathbf{1}^\top$ and $\mathbf{1}^\top p(0) = n * I(0)$, the average infection levels of the two models are identical. However, when the non-trivial network is employed, the results are quite different.

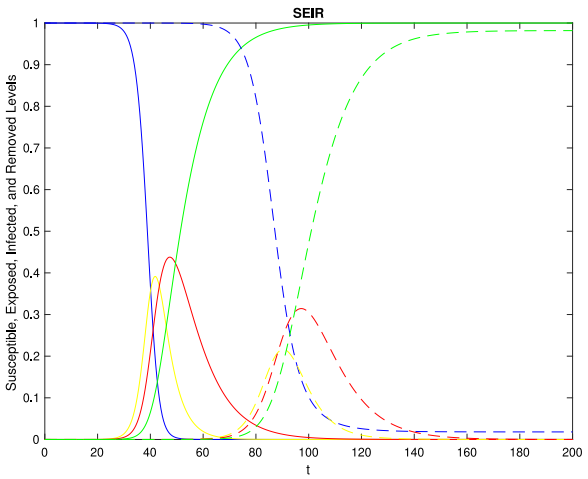

Fig. 8. SEIR simulation results. Blue, red, green, and yellow represent susceptible, infected, recovered (or removed), and exposed, respectively. The solid lines are the states of the group model in (3) and the dashed lines represent the average states of the networked model in (17).

For simplicity, we assume homogeneous spread for all of the models. We set $\beta = 1$, $\gamma = 0.1$, $\sigma = 0.2$, $\kappa = 0.143$, $\beta^E = 0.25$, and $q = 0.3$. The initial condition for the SIS and SIR models are

$$I(0) = 10^{-7} \text{ and } p(0)^\top = \begin{bmatrix} 0 & \cdots & 0 & 10^{-7} \end{bmatrix}, \tag{57}$$

which, for the networked model, assumes that the initial infected portion of the state comes from the downtown Chicago area, instead of being evenly distributed across the state. Similarly, the initial conditions for the SEIR and SAIR models are

$$E(0) = 10^{-7} \text{ and } e(0)^\top = \begin{bmatrix} 0 & \cdots & 0 & 10^{-7} \end{bmatrix} \tag{58}$$

and

$$A(0) = 10^{-7} \text{ and } a(0)^\top = \begin{bmatrix} 0 & \cdots & 0 & 10^{-7} \end{bmatrix}, \tag{59}$$

respectively. When not specified, the rest of the population is susceptible.

To illustrate the results we follow the color conventions from Figs. 1–4. That is, blue, red, green, yellow, and magenta represent susceptible, infected, recovered (or removed), exposed, and asymptomatic, respectively. We plot the proportions from the models in Section 2 and plot the averages of the states of the models in Section 3, all over time. The solid lines are for the group models from Section 2 and the dashed lines represent the average states of the networked models from Section 3. See Fig. 6 for the simulations of the SIS models. See Fig. 7 for the simulations of the SIR models. See Fig. 8 for the simulations of the SEIR models. Finally, see Fig. 9 for the simulations of the SAIR models.

Note that the simulation results are very different between the group models in Section 2 and the networked models in Section 3. The fully connected assumption of the group models leads to more drastic rates of increase and overall worse equilibria. Therefore, it is important to understand how subpopulations interact, that is, the underlying network, in order to be able to understand the spread of epidemics and to be able to design algorithms to mitigate their spread.

The parameter estimation techniques from Section 7 perform identically to (Paré et al., 2019; Vrabac, Paré et al., 2020) for the SIS model and in a similar manner for the rest of the models. When there is no noise, the parameters are recovered exactly. When noise is introduced, the estimation of the parameters is less accurate. See (Vrabac, Paré et al., 2020) for a more detailed exploration of the noisy cases.

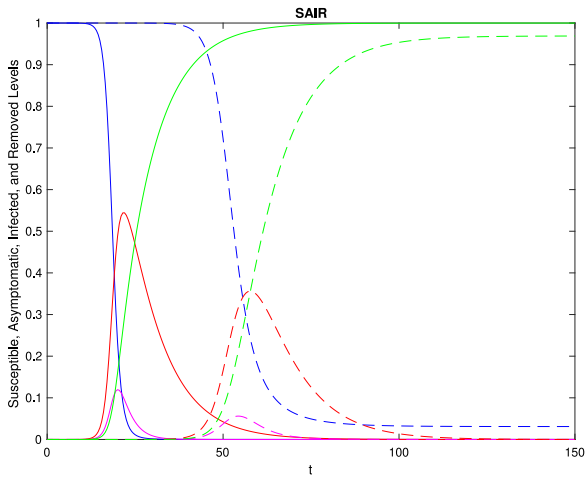

Fig. 9. SAIR simulation results. Blue, red, green, and magenta represent susceptible, infected, recovered (or removed), and asymptomatic, respectively. The solid lines are the states of the group model in (4) and the dashed lines indicate the average states of the networked model in (18).

As we stated before, leveraging these results on real data is a subject of ongoing work; see (Vrabac, Shang et al., 2020). We hope that other researchers can use this manuscript as a manual to help implement the ideas on their own datasets. In the context of the COVID-19 pandemic, it is important to have accurate models that do not overestimate the spread of the virus. Therefore, the networked models are quite important. However, on the other hand, obtaining clean data is a challenge, and, as the results in Section 7 show, estimating more model parameters requires more data and apriori information. Further, at certain levels of granularity, it may not be reasonable to assume that the network structure is known, and recovering network structure from time series is a difficult problem (Paré et al., 2013; Prasse & Van Mieghem, 2020). Therefore, researchers must balance these different challenges when choosing between group and networked epidemic models, depending on their data, apriori knowledge of the situation, and objectives.

9. Conclusion

In this paper we have presented various mathematical models of epidemic processes: SIS, SIR(S), SEIR(S), and SAIR(S). We first presented traditional group models for which no underlying graph structures are assumed, or the graph is trivial, that is, fully, and equally, connected. Then we presented continuous-time and discrete-time versions of the models with non-trivial networks. We presented stability analysis results for selected models from all three sets of models. We also presented least squares approaches for estimating the viral spreading parameters from data for each of the discrete-time networked models. We have also presented a set of simulations that illustrate how ignoring graph structure can lead to poor prediction of the growth and end result of outbreaks, supporting the need for networked models.

For future work we hope, and encourage others, to apply these ideas to different data sets to be able to understand outbreaks in different regions of the world. Exploring the case of parameter estimation in the presence of noise, with provable bounds, is an open problem, to the best of our knowledge, that should be worked on.

One class of problems in this context that our Overview has not addressed is active control of the spread of epidemics by directly manipulating the parameters that define the models, including weighting terms in the networked models. Several papers in the literature have addressed such issues, with some representative ones being (Enns et al., 2012; Khanafer & Başar, 2014a, 2014b; Mai et al., 2018; Preciado et al., 2014; Wan et al., 2008). Despite these existing works, developing provably optimal, distributed data-driven mitigation strategies is still a mostly open problem area. Additionally, some efforts are being explored to develop complete, closed-loop frameworks from testing data all the way through control implementation (Hota et al., 2020), but there is still much work to be done in this direction.

Declaration of competing interest

The authors declare that they have no known competing financial interests or personal relationships that could have appeared to influence the work reported in this paper.

Acknowledgments

The authors wish to thank Damir Vrabac for several useful discussions and contributions that improved the networked SAIR result given in Lemma 8 and many of the results in Section 7, Xiaoqi Bi for her contributions to the analysis of the group SAIRS model, and Erik Miehling for several insightful discussions related to this work.

References

Ahn, H. J., & Hassibi, B. (2013). Global dynamics of epidemic spread over complex networks. In *Proceedings of the IEEE Conference on Decision and Control* (pp. 4579–4585).

Anastassopoulou, C., Russo, L., Tsakris, A., & Siettos, C. (2020). Data-based analysis, modelling and forecasting of the COVID-19 outbreak. *PLoS One*, http://dx.doi.org/10.1371/journal.pone.0230405, [March].

Anderson, R. M., & May, R. (1992). *Infectious diseases of humans: Dynamics and control*. Oxford University Press.

Arcede, J. P., Caga-anan, R. L., Mentuda, C. Q., & Mammeri, Y. (2020). Accounting for symptomatic and asymptomatic in a SEIR-type model of COVID-19. arXiv preprint arXiv:2004.01805.

Atkinson, K. E. (2008). *An introduction to numerical analysis*. John Wiley & Sons.

Berman, A., & Plemmons, R. J. (1994). *Nonnegative matrices in the mathematical sciences*. SIAM.

Bernoulli, D. (1760). Essai d'une nouvelle analyse de la mortalité causée par la petite vérole et des avantages de l'inoculation pour la prévenir. *Histoire de l'Acad. Roy. Sci. avec Mém. des Math. et Phys. and Mém*, 1–45.

Bertozzi, A. L., Franco, E., Mohler, G., Short, M. B., & Sledge, D. (2020). The challenges of modeling and forecasting the spread of COVID-19. *Proceedings of the National Academy of Sciences of the United States of America*, http://dx.doi.org/10.1073/pnas.2006520117.

Boccaletti, S., Latora, V., Moreno, Y., Chavez, M., & Hwang, D.-U. (2006). Complex networks: Structure and dynamics. *Physics Reports*.

Chatterjee, S., & Durrett, R. (2009). Contact processes on random graphs with power law degree distributions have critical value 0. *The Annals of Probability*, (6), 2332–2356.

Cherif, A. (2015). Mathematical analysis of multiple strain, multi-locus-alele system for antigenically variable infectious diseases revisited. *Mathematical Biosciences*, 24–40.

Cheynet, E. (2020). Generalized SEIR epidemic model: fitting and computation. URL https://www.mathworks.com/matlabcentral/fileexchange/74545-generalized-seir-epidemic-model-fitting-and-computation. version 4.8.6.

Draief, M., & Massoulie', L. (2010). *Epidemics and rumours in complex networks*. Cambridge University Press.

Enns, E. A., Mounzer, J. J., & Brandeau, M. L. (2012). Optimal link removal for epidemic mitigation: A two-way partitioning approach. *Mathematical Biosciences*, *235*(2), 138–147.

Fall, A., Iggidr, A., Sallet, G., & Tewa, J. J. (2007). Epidemiological models and Lyapunov functions. *Mathematical Modelling of Natural Phenomena*, *2*(1), 62–83.

Giordano, G., Blanchini, F., Bruno, R., Colaneri, P., Di Filippo, A., Di Matteo, A., & Colanari, M. (2020). Modelling the COVID-19 epidemic and implementations of population-wide interventions in Italy. *Nature Medicine*.

Gracy, S., Paré, P. E., Sandberg, H., & Johansson, K. H. (2020). Analysis and distributed control of periodic epidemic processes. *IEEE Transactions on Control of Network Systems*.

Groendyke, C., & Combs, A. (2020). Modifying the network-based stochastic SEIR model to account for quarantine. arXiv preprint arXiv:2008.01202.

Grunnill, M. (2018). An exploration of the role of asymptomatic infections in the epidemiology of dengue viruses through susceptible, asymptomatic, infected and recovered (SAIR) models. *Journal of Theoretical Biology*, *439*, 195–204.

Hethcote, H. (2000). The mathematics of infectious diseases. *SIAM Review*, *42*(4), 599–653.

Hota, A. R., Godbole, J., Bhariya, P., & Paré, P. E. (2020). A closed-loop framework for inference, prediction and control of SIR epidemics on networks. *Annual Reviews in Control*, (submitted for publication). https://arxiv.org/abs/2006.16185.

Hota, A., & Sundaram, S. (2019). Game-theoretic vaccination against networked SIS epidemics and impacts of human decision-making. *IEEE Transactions on Control of Network Systems*, *6*(4), 1461–1472.

Illinois Department of Public Health (2020). Restore Illinois. https://www.dph.illinois.gov/restore. (Accessed 7 July 2020).

Kephart, J. O., & White, S. R. (1991). Directed-graph epidemiological models of computer viruses. In *Proceedings of the IEEE Symposium on Security and Privacy* (pp. 343–361).

Kermack, W. O., & McKendrick, A. G. (1932). Contributions to the mathematical theory of epidemics. II. The problem of endemicity. *Proceedings of the Royal Society of London, Series A (Mathematical and Physical Sciences)*, *138*(834), 55–83.

Khalil, H. K. (2002). *Nonlinear systems*. Prentice Hall.

Khanafer, A., Başar, T., & Gharesifard, B. (2016). Stability of epidemic models over directed graphs: a positive systems approach. *Automatica*, *74*, 126–134.

Khanafer, A., & Başar, T. (2014a). An optimal control problem over infected networks. In *Proceedings of the International Conference of Control, Dynamic Systems, and Robotics (CDSR14)*.

Khanafer, A., & Başar, T. (2014b). On the optimal control of virus spread in networks. In *Proc. International Conference on NETwork Games, COntrol and OPtimization* (pp. 166–172).

Khanafer, A., Başar, T., & Gharesifard, B. (2014a). Stability properties of infected networks with low curing rates. In *Proceedings of the American Control Conference* (pp. 3579–3584).

Khanafer, A., Başar, T., & Gharesifard, B. (2014b). Stability properties of infection diffusion dynamics over directed networks. In *Proceedings of the IEEE Conference on Decision and Control* (pp. 6215–6220).

Lajmanovich, A., & Yorke, J. A. (1976). A deterministic model for gonorrhea in a nonhomogeneous population. *Mathematical Biosciences*, *28*(3–4), 221–236.

Lewien, P., & Chapman, A. (2019). Time-scale separation on networks for multi-city epidemics. In *Proceedings of the IEEE 58th Conference on Decision and Control (CDC)* (pp. 746–751).

Li, M. Y., & Muldowney, J. S. (1995). Global stability for the SEIR model in epidemiology. *Mathematical Biosciences*, *125*(2), 155–164.

Liu, F., Cui, S., Li, X., & Buss, M. (2020). On the stability of the endemic equilibrium of a discrete-time networked epidemic model. In *Proceedings of the IFAC World Congress* (pp. 1–6).

Liu, J., Paré, P. E., Nedić, A., Tang, C. Y., Beck, C. L., & Başar, T. (2019). Analysis and control of a continuous-time bi-virus model. *IEEE Transactions on Automatic Control*, *64*(12), 4891–4906.

Liu, C., Wu, X., Niu, R., Wu, X., & Fan, R. (2020). A new SAIR model on complex networks for analysing the 2019 novel coronavirus (COVID-19). *Nonlinear Dynamics*, 1–11.

Mai, V., Battou, A., & Mills, K. (2018). Distributed algorithm for suppressing epidemic spread in networks. *IEEE Control Systems Letters*, *2*(3), 555–560.

Mallapaty, S. (2020). Antibody tests suggests coronavirus infections vastly exceed official counts. *Nature, News Article*.

Mei, W., Mohagheghi, S., Zampieri, S., & Bullo, F. (2017). On the dynamics of deterministic epidemic propagation over networks. *Annual Reviews in Control*, *44*, 116–128.

Mena-Lorca, J., & Hethcote, H. (1992). Dynamic models of infectious diseases as regulators of population size. *Journal of Mathematical Biology*, *30*, 693–716.

Mieghem, P. V., & Omic, J. (2014). In-homogeneous virus spread in networks. arXiv preprint arXiv:1306.2588v2.

Mieghem, P. V., Omic, J., & Kooij, R. (2009). Virus spread in networks. *IEEE/ACM Transactions on Networking*, (1), 62–68.

Norris, J. R. (1998). *Markov chains, vol. 2*. Cambridge University Press.

Nowzari, C., Preciado, V. M., & Pappas, G. J. (2014). Stability analysis of generalized epidemic models over directed networks. In *Proceedings of the IEEE conference on decision and control* (pp. 6197–6202).

Nowzari, C., Preciado, V. M., & Pappas, G. J. (2016). Analysis and control of epidemics: A survey of spreading processes on complex networks. *IEEE Control Systems Magazine*, (1), 26–46.

Pagliara, R., & Leonard, N. E. (2020). Adaptive susceptibility and heterogeneity in contagion models on networks. *IEEE Transactions on Automatic Control*, 1.

Pare, P. E. (2018). Virus spread over networks: Modeling, analysis, and control (Ph.D. thesis), University of Illinois at Urbana-Champaign.

Paré, P. E., Beck, C. L., & Nedić, A. (2018). Epidemic processes over time-varying networks. *IEEE Transactions on Control over Network Systems*, (3), 1322–1334.

Paré, P. E., Chetty, V., & Warnick, S. (2013). On the necessity of full-state measurement for state-space network reconstruction. In *Proceedings of the 2013 IEEE Global Conference on Signal and Information Processing* (pp. 803–806).

Paré, P. E., Liu, J., Beck, C. L., & Başar, T. (2019). Networked infectious disease–contaminated water model. In *Proceedings of the 2019 18th European Control Conference (ECC)* (pp. 2018–2023).

Paré, P. E., Liu, J., Beck, C. L., Kirwan, B. E., & Başar, T. (2019). Analysis, identification, and validation of discrete-time epidemic processes. *IEEE Transactions on Control Systems Technology*, *28*(1), 79–93.

Pastor-Satorras, R., Castellano, C., Van Mieghem, P., & Vespignani, A. (2015). Epidemic processes in complex networks. *Reviews of Modern Physics*, *87*(3), 925.

Pires, M. A., Oestereich, A. L., & Crokidakis, N. (2018). Sudden transitions in coupled opinion and epidemic dynamics with vaccination. *Journal of Statistical Mechanics: Theory and Experiment*, (5), Article 053407.

Prasse, B., & Van Mieghem, P. (2020). Network reconstruction and prediction of epidemic outbreaks for general group-based compartmental epidemic models. *IEEE Transactions on Network Science and Engineering*, 1.

Preciado, V. M., Zargham, M., Enyioha, C., Jadbabaie, A., & Pappas, G. (2014). Optimal resource allocation for network protection: A geometric programming approach. *IEEE Transactions on Control of Network Systems*, *1*(1), 99–108.

Rogers, E. M. (2003). *Diffusion of innovations* (fifth ed.). Free Press.

Rohloff, K. R., & Başar, T. (2008). Deterministic and stochastic models for the detection of random constant scanning worms. *ACM Transactions on Modeling and Computer Simulation*, *18*(2), 8:1–8:24.

Roosa, K., & Chowell, G. (2019). Assessing parameter identifiability in compartmental dynamic models using a computational approach: application to infectious disease transmission models. *Theoretical Biology and Medical Modelling*, *16*(1), 1.

Rothe, C., Schunk, M., Sothmann, P., Bretzel, G., Froeschl, G., Wallrauch, C., Zimmer, T., Thiel, V., Janke, C., Guggemos, W., et al. (2020). Transmission of 2019-nCoV infection from an asymptomatic contact in Germany. *New England Journal of Medicine*, *382*, 970–971.

Silver, N. (2020). Coronavirus case counts are meaningless. *FiveThirtyEight*.

Snow, J. (1855). *On the mode of communication of cholera*. John Churchill.

Van Mieghem, P. (2014). Exact Markovian SIR and SIS epidemics on networks and an upper bound for the epidemic threshold. arXiv preprint arXiv:1402.1731.

Van Mieghem, P., Omic, J., & Kooij, R. (2009). Virus spread in networks. *IEEE/ACM Transactions on Networking*, *17*(1), 1–14.

Vrabac, D., Paré, P. E., Sandberg, H., & Johansson, K. H. (2020). Overcoming challenges for estimating virus spread dynamics from data. In *Proceedings of the 54th Annual Conference on Information Sciences and Systems (CISS)*.

Vrabac, D., Shang, M., Pham, J., Stern, R., & Paré, P. E. (2020). Networked SIR & SEIR models to capture the effects of transportation on the spread of COVID-19. In *Submission to IEEE Control Systems Letters & the 2021 American Control Conference*.

Wan, Y., Roy, S., & Saberi, A. (2007). Network design problems for controlling virus spread. In *Proceedings of the 46th IEEE Conference on Decision Control* (pp. 3925–3932).

Wan, Y., Roy, S., & Saberi, A. (2008). Designing spatially heterogeneous strategies for control of virus spread. *IET Systems Biology*, *2*(4), 184–201.

Wang, Y., Chakrabarti, D., Wang, C., & Faloutsos, C. (2003). Epidemic spreading in real networks: an eigenvalue viewpoint. In *Proceedings of the 22nd International Symposium on Reliable Distributed Systems* (pp. 25–34).

World Health Organization (WHO), a. Coronavirus (COVID-19) outbreak. https://www.who.int/westernpacific/emergencies/covid-19. (Accessed 7 July 2020).

World Health Organization (WHO), b. Ebola virus disease – Democratic Republic of the Congo. https://www.who.int/csr/don/26-June-2020-ebola-drc/en/. (Accessed 7 July 2020).

Yoon, D., & Martin, D. (2020). South Korea's new coronavirus twist: recovered patient's test positive again. *Wall Street Journal*.

Philip E. Paré is an Assistant Professor in the School of Electrical and Computer Engineering at Purdue University. He received his Ph.D. in Electrical and Computer Engineering from the University of Illinois at Urbana-Champaign in 2018, after which he went to KTH Royal Institute of Technology in Stockholm, Sweden to be a Post-Doctoral Scholar from 2019–2020. He received his B.S. in Mathematics with University Honors and his M.S. in Computer Science from Brigham Young University in 2012 and 2014, respectively. At the University of Illinois, he was the recipient of the Robert T. Chien Memorial Award for excellence in research

and named a Mavis Future Faculty Fellow. His research focuses on networked control systems, namely modeling, analysis, and control of virus spread over networks.

Carolyn L. Beck is a Professor at the University of Illinois, Urbana-Champaign (UIUC) in the Industrial and Enterprise Systems Engineering (ISE) Department. She completed her Ph.D. at Caltech, her M.S. at Carnegie Mellon, and her B.S. at Cal Poly, all in Electrical Engineering. Prior to completing her Ph.D., she worked at Hewlett-Packard in Silicon Valley, designing digital hardware and software for measurement instruments. She has held visiting faculty positions at the Royal Institute of Technology (KTH) in Stockholm, Stanford University in Palo Alto and Lund University in Lund, Sweden. She has received national research awards and local teaching awards. Prof. Beck's research interests range from network inference problems to control of anesthetic pharmacodynamics. Her main research interests are in mathematical modeling, analysis and control of network systems; model reduction and approximation; and clustering and aggregation methods applied to data from network systems.

Tamer Başar is with the University of Illinois at Urbana-Champaign (UIUC), where he holds the academic positions of Swanlund Endowed Chair; Center for Advanced Study Professor of Electrical and Computer Engineering; Research Professor at the Coordinated Science Laboratory; and Research Professor at the Information Trust Institute. He is also the Director of the Center for Advanced Study. He received B.S.E.E. from Robert College, Istanbul, and M.S., M.Phil, and Ph.D. from Yale University. He is a member of the US National Academy of Engineering, and Fellow of IEEE, IFAC and SIAM, and has served as president of IEEE CSS, ISDG, and AACC. He has received several awards and recognitions over the years, including the highest awards of IEEE CSS, IFAC, AACC, and ISDG; the IEEE Control Systems Award; and a number of international honorary doctorates and professorships. He has over 900 publications in systems, control, communications, and dynamic games, including books on non-cooperative dynamic game theory, robust control, network security, wireless and communication networks, and stochastic networked control. He was the Editor-in-Chief of Automatica between 2004 and 2014, and is currently editor of several book series. His current research interests include stochastic teams, games, and networks; security; and cyber–physical systems.